LOCKHEED MARTIN

LOCKHEED MARTIN CORPORATION
Missiles & Space
3251 Hanover Street
Palo Alto, California 94304-1191

In reply refer to:
LMMS/VMD-98-201

June 16, 1998

National Aeronautics and Space Administration
Goddard Space Flight Center
Greenbelt Road
Greenbelt, Maryland 20771

IN-90
37176

Attention: Mr. James Debilious, Code 216

Subject: Purchase Order No. S-68399F
An Investigation of the Largest Flares
in Active Cool Star Binaries with ALEXIS

Reference: Article C.2

Enclosure: One (1) Copy Final Report

Dear Mr. Debilious:

LMMS is pleased to enclosethe Final Report for the subject purchase order.

Please contact the undersigned at (650) 424-2001, if you have any questions. Further correspondence may be addressed to the attention of the undersigned at Organization 25-62, Building 255, at the above Palo Alto address. Our 24-hour facsimile number is (415) 424-3333.

LOCKHEED MARTIN CORPORATION
Missiles & Space

Virginia M. Dougherty
Contract Administrator
Advanced Technology Center

cc: NASA/GSFC:
D. West, Code 684 (w/encl.)
Publication and Graphics Services Section, Code 253.1 (w/encl.)

NASA Center for Aerospace Information (CASI)
7121 Standard Drive
Hanover, MD 21076-1320
Attn: Acquisitions Department (w/encl.)

An Investigation of the Largest Flares in Active Cool Star Binaries with ALEXIS

NASA P.O. No. S- 68399-F

Final Report

Submitted To:

National Aeronautics and Space Administration
Goddard Space Flight Center
Greenbelt MD 20771

Principal Investigator:

Robert A. Stern
Dept H1-12 Bldg 252
Solar and Astrophysics Laboratory
Lockheed Martin ATC
3251 Hanover St.
Palo Alto, CA 94304
(415) 424-3272

June 3, 1998

1. Summary

We proposed to search for high-temperature, flare-produced Fe XXIII line emission from active cool star binary systems using the ALEXIS all-sky survey. Previous X-ray transient searches with ARIEL V and HEAO-1, and subsequent shorter duration monitoring with the *GINGA* and *EXOSAT* satellites demonstrated that active binaries can produce large (EM $\approx 10^{55-56}$ cm^{-3}) X-ray flares lasting several hours or longer. Hot plasma from these flares at temperatures of 10^7 K or more should produce Fe XXIII line emission at $\lambda = 132.8$Å, very near the peak response of ALEXIS telescopes 1A and 2A. Our primary goals were to estimate flare frequency for the largest flares in the active binary systems, and, if the data permitted, to derive a distribution of flare energy vs. frequency for the sample as a whole.

After a long delay due to the initial problems with the ALEXIS attitude control, the heroic efforts on the part of the ALEXIS satellite team enabled us to carry out this survey. However, the combination of the higher than expected and variable background in the ALEXIS detectors, and the lower throughput of the ALEXIS telescopes resulted in no convincing detections of large flares from the active binary systems. In addition, vignetting-corrected effective exposure times from the ALEXIS aspect solution were not available prior to the end of this contract; therefore, we were unable to convert upper limits measured in ALEXIS counts to the equivalent L_{EUV}.

2. Technical Progress

2.1 Background

X-ray emission from RS CVn and related active binary systems is commonly known to be much stronger than from typical single star coronae (Pallavicini 1989; also see the Strassmeier *et al.* 1993catalog and references therein). These same systems also produce some of the largest known stellar flares in terms of X-ray luminosity or emission measure. Stern (1991) reviewed recent studies of X-ray flaring in such systems: Figure 1 from this paper is reproduced below.

A quick inspection of Figure 1 reveals several important facts: (1) even the largest solar flares pale in comparison to the largest RS CVn flares, (2) the classical "flare stars" also fail, by orders of magnitude, to reproduce the emission measures of the RS CVn flares, and (3) at least in terms of X-ray continuum temperature, the largest flares also seem to have the highest temperatures.

There were a limited number of RS CVn flares seen with *Einstein*, including one on σ^2 CrB (Agrawal *et al.* 1981), and another on the RS CVn-like Hyades binary HD 27130 (Stern *et al.* 1983). However, the most detailed studies of stellar flare properties in active systems were made with *EXOSAT*, and, more recently, *GINGA*. Flares in the active binary systems σ^2 CrB , II Peg, TY Pyx, and Algol were seen by *EXOSAT* (see review by Pallavicini 1989). Some of the brightest X-ray flares were observed with the

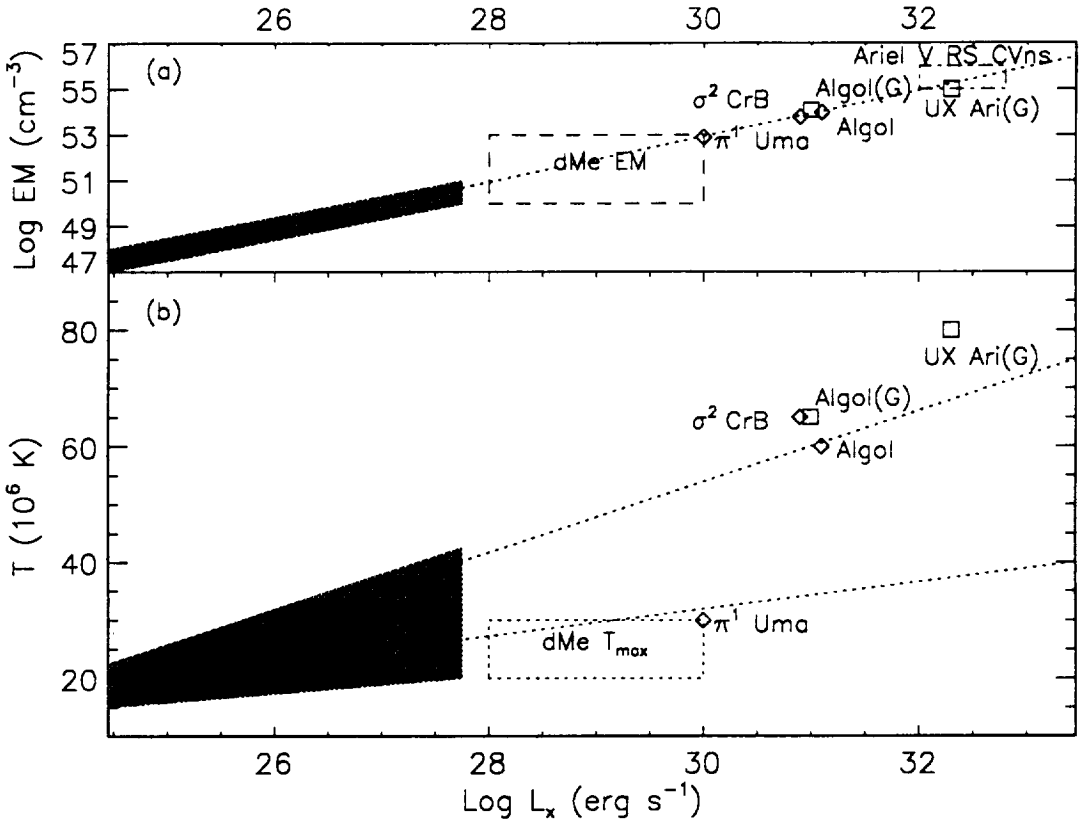

Figure 1: (a) Emission measure ($n_e^2 V$) vs L_x for a variety of solar and stellar flares (G=*GINGA* data). Approximate ranges for dMe flares and a group of large RS CVn flares seen by Ariel V are shown. The L_x vs EM relation estimated by Tanaka(1987) for solar flares is shown as a dotted line. (b) Similar plot for flare temperature. The approximate relations for "high T" and "low T" solar flares suggested by Tanaka (1987) are shown as dotted lines. In both plots, shaded region indicates approximate range of solar data.

GINGA satellite in UX Ari (Tsuru *et al.* 1989), II Peg (Doyle *et al.* 1991) and Algol (Stern *et al.* , 1992). A summary of large flares seen in RS CVn systems is given in Table 1.

Despite their limited number, the EXOSAT and *GINGA* observations yield important constraints on flare physical parameters, including temperatures, cooling times, densities, and size scales. There is, however, considerably less knowledge regarding flare frequency in such systems. This is simply because the vast majority of information we have regarding stellar X-ray flares was obtained with *pointed* instruments on *Einstein, EXOSAT, and Ginga.* Yet events with an emission measure (EM=$n_e^2 V$) $> 10^{54}$ cm^{-3} cannot be too rare; otherwise, the success rate for detecting flares in the very limited number of several-day pointed observations would be nil. As in the case of solar flares,

Table 1: Largest Flares Reported for RS CVn Systems and Algol

System	L_x[a]	Reference
σ^2 CrB *(EXOSAT)*	≈ 5	van den Oord *et al.* (1988)
HR 1099 (Copernicus)	22	White *et al.* (1978)
HR 1099 (Ariel V)	600	Pye and McHardy (1983)
UX Ari (Ariel V)	600	Pye and McHardy (1983)
UX Ari (em GINGA)	120	Tsuru *et al.* (1989)
AR Psc (HEAO-1)	250	Ambruster and Wood (1986)
II Peg (Ariel V)	150	Pye and McHardy (1983)
II Peg (em GINGA)	30	Doyle *et al.* (1991)
σ Gem (Ariel V)	400	Pye and McHardy (1983)
Algol *(EXOSAT)*	≈ 10	White *et al.* (1986)
Algol (em GINGA)	10	Stern *et al.* (1990)

[a] $10^{30}\ erg\ s^{-1}$, 2–10 keV

there is likely to be a "log N–log S" type relation for flare frequency vs energy: on the Sun, the number of X-ray bursts above a given threshold scales roughly as S^{-1}, where S is the peak energy flux (e.g., Drake 1971). At this time, there are simply too few observations to determine such a relationship for active binary X-ray flares; what little data exist are from X-ray transient surveys.

Although there have been many studies of X-ray transients, the two most sensitive, and therefore most useful in estimating flare rates, were the Ariel V SSI all sky transient survey (Pye and McHardy 1983) and the HEAO-1 A-1 all sky transient survey (Ambruster and Wood 1986). The HEAO-1 survey had a sensitivity limit of $\approx 10^{-10}$ erg cm^{-2} s^{-1} in the 0.5-20 keV range, while the Ariel V sensitivity limit (for a single orbit) was $\approx$ 3-4 $\times$ 10^{-10} erg cm^{-2} s^{-1} in the 2-18 keV band. At a distance of 50 pc, these sensitivity limits correspond to 3 $\times$ 10^{31} to $> 10^{32}$ erg s^{-1}. Both studies were carried out with scanning collimated proportional counters: the HEAO-1 instrument had a 1° $\times$ 4° FOV, and the Ariel V SSI a 0.75° $\times$ 10.6° FOV. Both missions operated in a sky scanning mode, with the long axis of the instrument field of view either perpendicular (HEAO-1) or highly inclined (Ariel V: 65°) to the spin plane.

Both experiments have detected the largest stellar flares observed to date (Table 1). A typical position in the sky was in the detector field of view only a limited number of days per year (up to 20 in the case of Ariel V, only 8 or so for the 7 months of the HEAO-1 A-1 survey). In spite of this, at least one of the HEAO-1 and six of the Ariel V transients were identified with RS CVn flares with $L_x = 10^{32-33}$ erg s^{-1} (Ambruster and Wood 1986, Pye and McHardy 1983). In the temperature range 20–60 x 10^6 K, typical for the X-ray emitting plasma in such flares, the 2–10 keV band emissivity is $\approx$ 5 $\times$ 10^{-24} to 10^{-23} erg cm^3 s^{-1} (Mewe, Gronenschild, and van den Oord 1985). Hence the

EM for these flares is $\approx 10^{55-56}$ cm^{-3} (see Figure 1). Pye and McHardy (1983) also note that the typical duration of the Ariel V flares is $\sim$ 3 orbits, or roughly 5 hours, with the notable exception of a 12 hour flare on σ Gem. A more recent example of a long flare is the moderately large (EM$\approx 10^{54}$ cm^{-3}) Algol event seen by *GINGA*, with an exponential decay time of $\approx$ 10 hours (Stern *et al.* 1990), as shown in Figure 2.

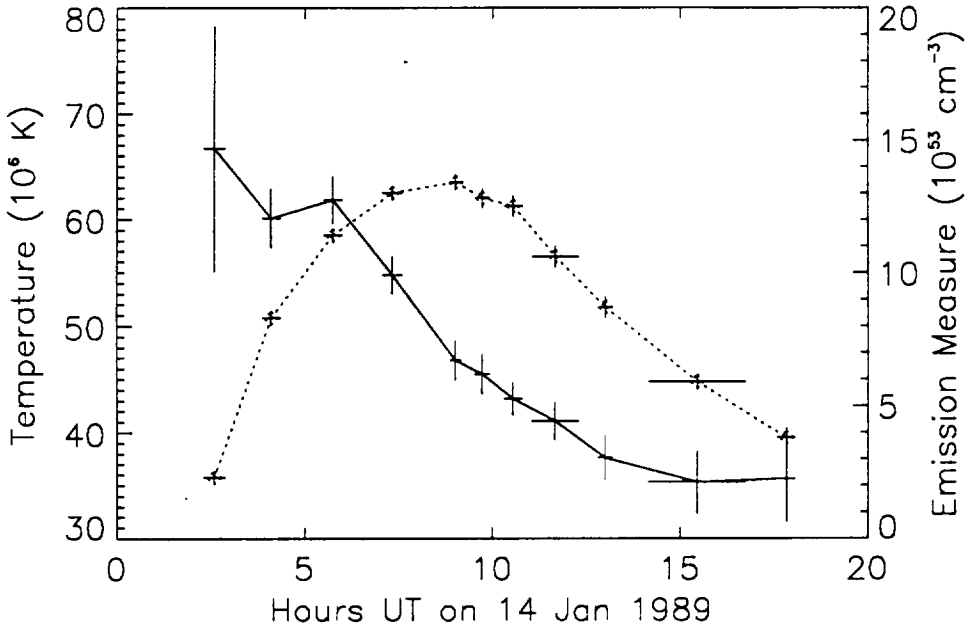

Figure 2: Temperature (solid line) and emission measure (dotted line) vs. time during Algol flare seen by *GINGA* (From Stern *et al.* 1990).

All the above results lead us to the conclusion that large flares are occurring with enough regularity on active binaries to classify them as true "flare stars," but on a much grander scale than the classical dMe systems. The long flare duration and huge emission measures also provide evidence that detection of similar or even fainter flares will be possible using the ALEXIS multilayer telescopes. Plasma at temperatures in the 10^7 K and higher range produce line emission, not only at X-ray wavelengths, but also in the EUV. In particular, the Fe XXIII line at 132.8 Å has a peak emissivity near $10^{7.2}$ K (Mewe, Gronenschild, and van den Oord 1985, Landini and Monsignori-Fossi 1990). Hence the cooling flare plasma from large X-ray flares should be seen as an increase in count rate in the 93 eV (130Å) band of ALEXIS.

2.2 ALEXIS Launch Problems and Recovery

Although this program was first proposed in 1992, and ALEXIS was launched in 1993, funding was delayed until March 1996 because of ALEXIS launch problems and the usual contractual delays. At some point during the ALEXIS launch, one of the brackets holding a solar panel (and magnetometer) to the ALEXIS spacecraft was broken. This prevented the satellite from properly acquiring the Sun during its start-up phase, and almost (but not quite) draining the batteries. As the ALEXIS orbit precessed, the position of the solar arrays relative to the Sun gradually changed, allowing initial acquisition of the satellite roughly two months after launch.

Remarkably, the solar panel with the broken attachment is still attached to the spacecraft via its wire bundle; however, this loose attachment has resulted in a significant "wobble" to the spin stabilized satellite and the need for constant ground adjustment of the spin axis orientation(Roussel-Dupré et. et. 1997). Hence significant effort was required to obtain attitude solutions. These efforts were successful, and ALEXIS is able to obtain positions of several bright steady EUV sources (such as HZ43) to $\sim$ 0.2 deg.

2.3 In-Orbit Performance

The in-orbit performance is not as good as expected pre-launch because of a number of factors:

(1) Telescopes 1A and 2A have roughly 60% of the response expected from pre-flight models (however, much of this is due to a narrower bandpass, which is only of significance for off-peak wavelengths)

(2) ALEXIS discovered a significant in-orbit background correlated with the ram angle of the satellite in orbit which results in background levels thousands of times greater than predicted. However, this background is present only during roughly 50% of each orbit; thus "good times" can be selected from the data, albeit with the effective exposure times per orbit reduced significantly, thus decreasing the sensitivity.

The sensitivity of the individual ALEXIS telescopes to coronal plasma is for an emission measure of 10^{52} cm^{-3} at 10 pc is shown in Figure 3.

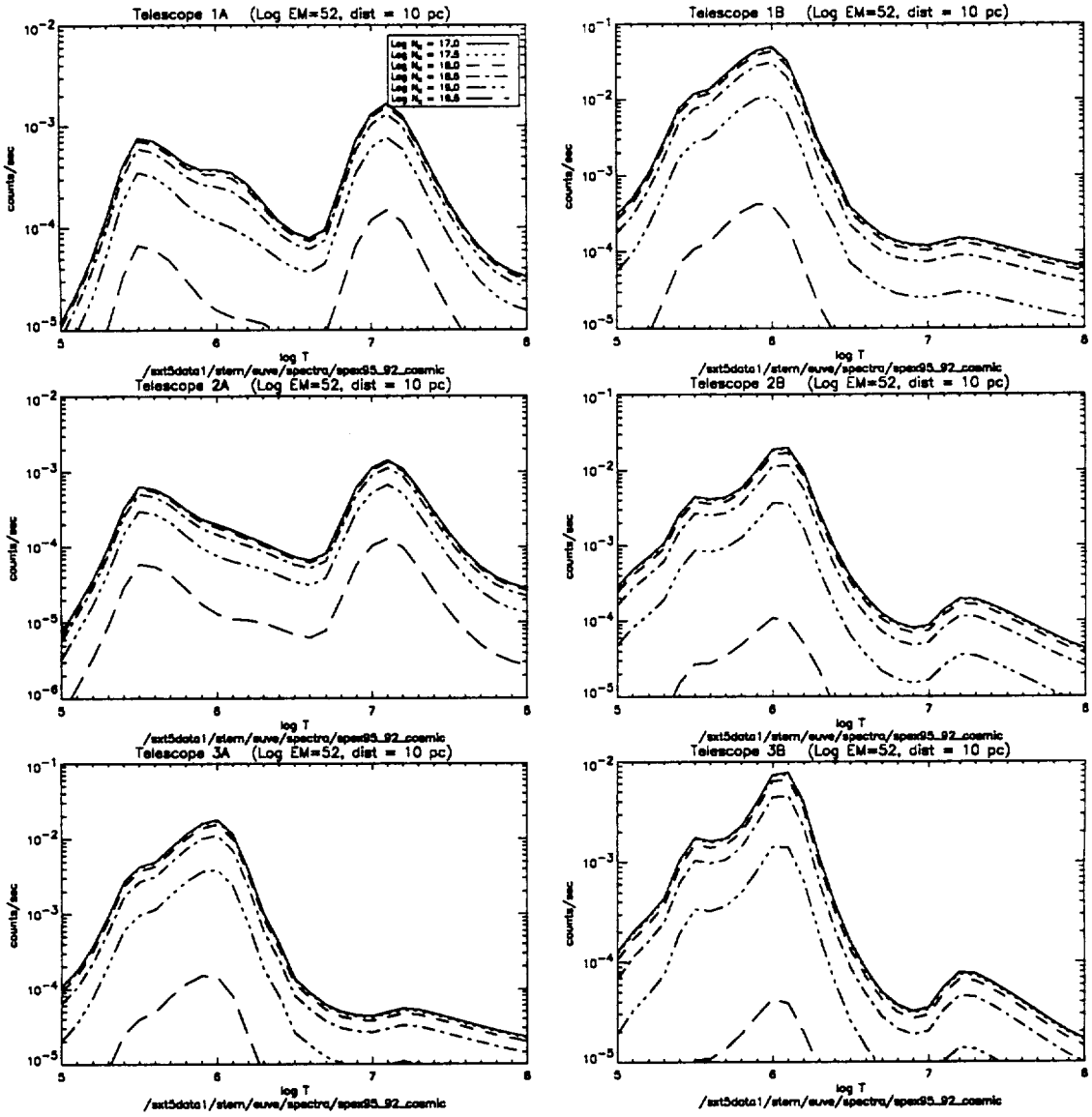

Figure 3: ALEXIS Sensitivity

2.4 Data Processing Approach

The data processing approach for this project differed somewhat from that adapted for the "standard" ALEXIS transient searches. Specifically, (1) the target list was known *a priori*, and (2) the time scales expected for the peak emission of large stellar flares were expected to be $\sim$ one to several ALEXIS orbits. Thus summing observations over a day or more (used in the case of some transient searches) would actually *reduce* the signal-to-noise of the observation. During a meeting at Los Alamos in April 1996, we

(J. Bloch and the LANL/ALEXIS team, X. Wu of the UCB/ALEXIS team and myself) agreed upon a modified strategy to detect stellar flares:

- For each target, a "pigeonhole" of aspect-corrected photon events was generated in sky coordinates with a 5° radius and 0.25° pixels.
- Each "pigeonhole" consisted of data taken in each of the 6 telescopes from December 1994 to April 1996.
- The event list was corrected to include only times of low anomalous background.
- For each "pigeonhole", a source region of 30 arc-min radius and a background annulus from 50-200 arc-min radii were chosen to test for the presence of a source using the method of Lampton (1994).
- The Lampton "score" for a single orbits worth of data and sums up to the 8 prior orbits were calculated and tabulated.
- As a statistical test of the technique, artificial data sets were generated using the same photon data but the aspect information rotated by 180° in the sky.
- As a test of the "efficiency" of the search techniques, we included in the target list a few sources known to have been previously detected in quiescence by the standard ALEXIS source detection algorithm: e.g. HZ43.

2.5 Target List

The list of targets used to create pigeonholes is given in Appendix A. The list consist of essentially all the objects in the Strassmeier *et al.* (1993) catalog. In addition, we included in the list the EUVE bright sources mentioned above, four nearby Algol systems, and (for another project headed by S. Cully using the same data set), a list of nearby flare stars and two cataclysmic variables. Results from the latter sources were ignored in the following analysis.

2.6 Results

Comparison of Original and "Rotated" Data Sets

The bright EUV sources put in our target list as test cases were successfully detected in quiescence by our transient search algorithm. At first, we also thought that one or more transients had been detected at a high level of significance: however, some detective work by Jeff Bloch demonstrated that these obvious detections were, in fact, due to reflected solar EUV radiation from the Moon.

After removal of the "test" detections from the EUV bright source list and the serendipitous lunar EUV detections, we examined the histogram of Lampton scores for

a portion of the data set. This consisted of roughly 120,000 single orbits of data, divided unequally among the 6 telescopes. We added together the telescope combinations with the same bandpasses (1A+2A, 1B+3A, and 2B+3B), and compared the actual data set with one whose aspect information had been artificially rotated by 180° about the telescope spin axis, thus, in principal providing a control sample to check the detection statistics. For each single orbit, we also added up the previous 2-9 orbits with acceptable data for each "pigeonhole", in an attempt to check our ability to detect longer transients. The results of this series of tests is presented graphically in Appendix A, Figures 1-9. Note that, in essentially all cases, the original and 180° rotated data sets produce the same distribution, with no Lampton Scores above 6.0. Recall that we have removed all "bright" steady sources such as HZ43 and the few objects known to be contaminated by the Moon. Thus, there is no strong evidence for a non-statistical distribution of transient sources with this portion of the data set.

Histograms of All Processed Data

Continuing in the above vein, we processed all the data then available. This represented approximately 16 months worth of data, or $\sim 1.6\times10^6$ telescope-orbit combinations. Hence, any detections significantly above a Lampton Score of about 6.0 for single orbit data should be clear transients. Once again, we summed up to 9 previous orbits to search for longer time scale events: note that the latter searches are not independent of the single orbit seraches or of each other. The results of these searches is shown in Figures 1-9 of Appendix B. In this case, we detected a number of events above the Lampton Score = 6.0 value; for single-orbit seraches, we would expect about 1, so, at first glance, the results look promising. However, a number of these "detections" are also lunar detections for objects such as V471 Tau and BD 17° +703. After removal of these, we detect about 5 objects above the 6.0 threshold. Since this includes all the multiple orbit searches, such a number is not particularly significant. Thus we are forced to conclude that ALEXIS has not detected any coronal transients with a high level of confidence.

Conversion to Flux Upper Limits

Given the above null result, we still could convert our data to provide upper flux limits in each of the telescope bands for our search. However, the software and processing required to determine effective exposure time and vignetting corrections to convert the counts into erg cm^{-2} s^{-1} was still in the process of being developed at the UCB ALEXIS Data Center at the time of completion of this contract. The data are still available, so that this task could be completed at a later date.

2.7 Summary and Conclusions

We searched $\approx$ 16 months of ALEXIS data for coronal flare-like transients, but obtained no unambiguous detections. The quantitative conversion of our results into upper limits awaits the completion of ALEXIS effective exposure software.

2.8 Acknowledgements

R.A.S. is indebted to Jeff Bloch, Diane Rousel-Dupré, James Theiler and the rest of the ALEXIS team at LANL for their input, expertise, support and hospitality, in particular during a visit to LANL to begin this program. In addition, we wish to thank Ozzie Siegmund and the ALEXIS Data Center staff at UCB, where most of the data processing occurred, for their support, especially Xiaoyi Wu, who wrote most of the processing code and produced the data sets which R.A.S. then analyzed. We are also very grateful to Scott Cully who, while completing his graduate thesis on another subject, provided much help and managed the overall coordination at UCB.

References

Agrawal, P.C., Riegler, G.R., and White, N.E., 1981, M.N.R.A.S, **196**, 73P.

Ambruster, C.W., and Wood, K.S., 1986, Ap.J., **311**, 258.

Drake, J.F., 1971, Sol. Phys., **16**, 152.

Doyle *et al.* 1991, M.N.R.A.S., **248**, 503.

Garcia, M., *et al.* , 1980, Ap. J. (Letters), **240**, L107.

Lampton, M., 1994, Ap. J., 436, 784.

Landini, M. and Monsignori-Fossi, B.C., 1990, Atron. Astrophys. Suppl., **82**, 229.

Mewe, R., Gronenschild, E.H.B.M., and van den Oord, G.H.J., 1985, Astron. Astrophys. Suppl., **62**, 197.

Pallavicini, R., 1989, *Astron. Astrophys. Rev.*, **1**, 177.

Pye, J.P., and McHardy, I.M., 1983, M.N.R.A.S., **205**, 875.

Rousel-Dupré, D., *et al.*, 1997, in 11th AIAA/USU Conference on Small Satellites (preprint).

Strassmeier, K.G.,*et al.*, 1993, Astron. Astrophys. Suppl., **100**, 173.

Stern, R.A., Haisch, B.M., Nagase, F., Uchida, Y. and Tsuneta, S., 1990, in *Cool Stars, Stellar Systems and the Sun: Sixth Cambridge Workshop*, ed. G. Wallerstein, Astron. Soc. Pac. Conf. Series **9**, 224.

Stern, R.A., 1991, Proceedings of the 28th Yamada Conference, *Frontiers of X-Ray Astronomy*, ed. K. Koyama, Universal Academy Press, Tokyo, p.259.

Stern, R.A., Underwood, J.H., and Antiochos, S.K., 1983, Ap. J. (Letters) , **264**, L55.

Stern, R.A., Uchida, Y., Tsuneta, S., and Nagase, F., 1992, Ap. J., **400**, 321.

Tanaka, K., 1987, PASJ, **39**, 1.

Tsuru, T.,*et al.*, 1989, Pub. Astron. Soc. Japan, **41**, 679.

White, N.E., Sanford, P.W., and Weiler, E.J., 1978, Nature, **274**, 569.

White, N.E., *et al.* , 1986, Ap.J., **301**, 262.
van den Oord, G.H.J., Mewe, R., and Brinkman, A.C., 1988, Astron. Astrophys., **205**, 181.

Appendix A

Comparison Histograms: Original and 180° Data Sets

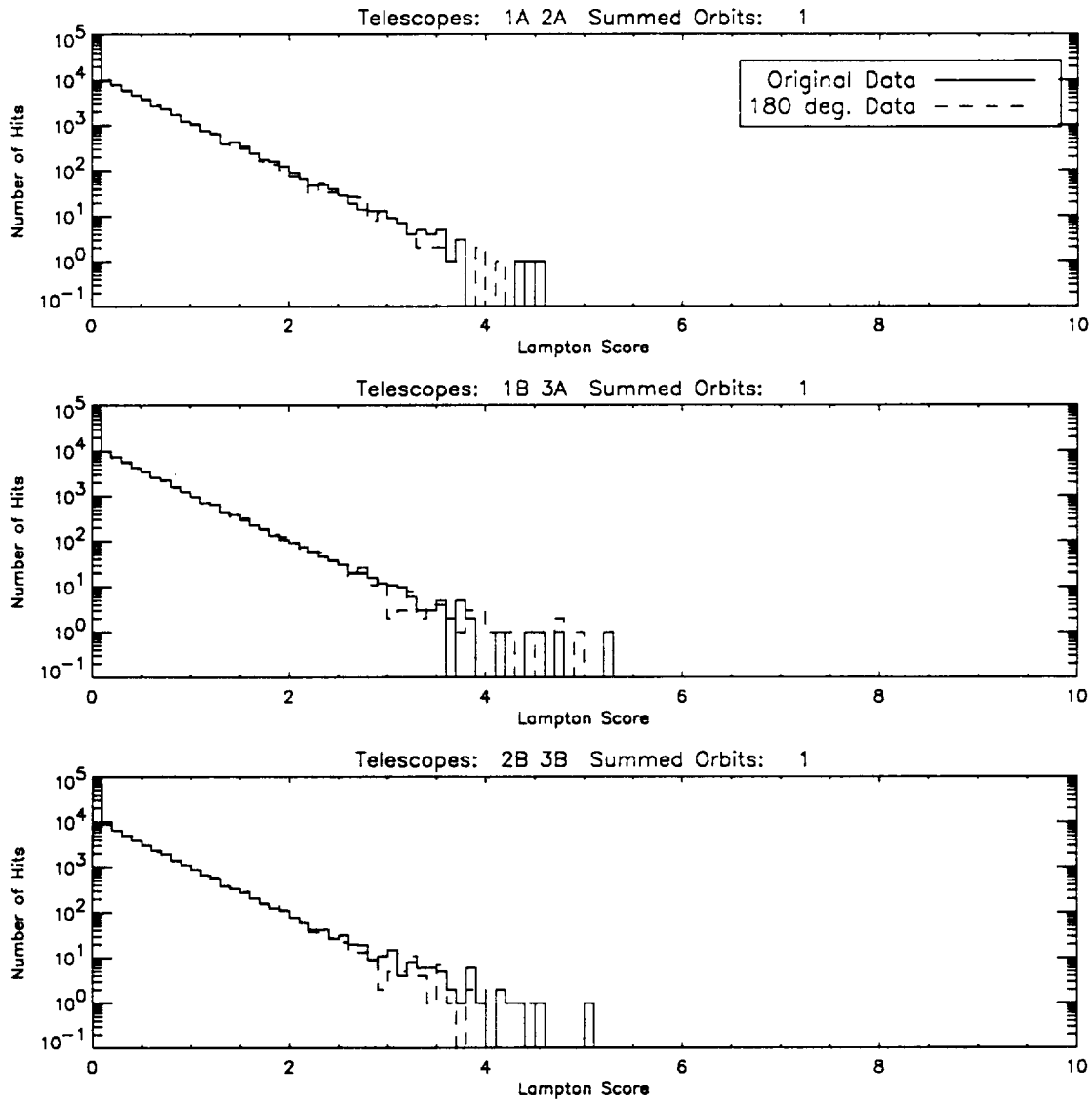

Figure 1: Comparison of Original and 180° Data: 1 Orbits Summed

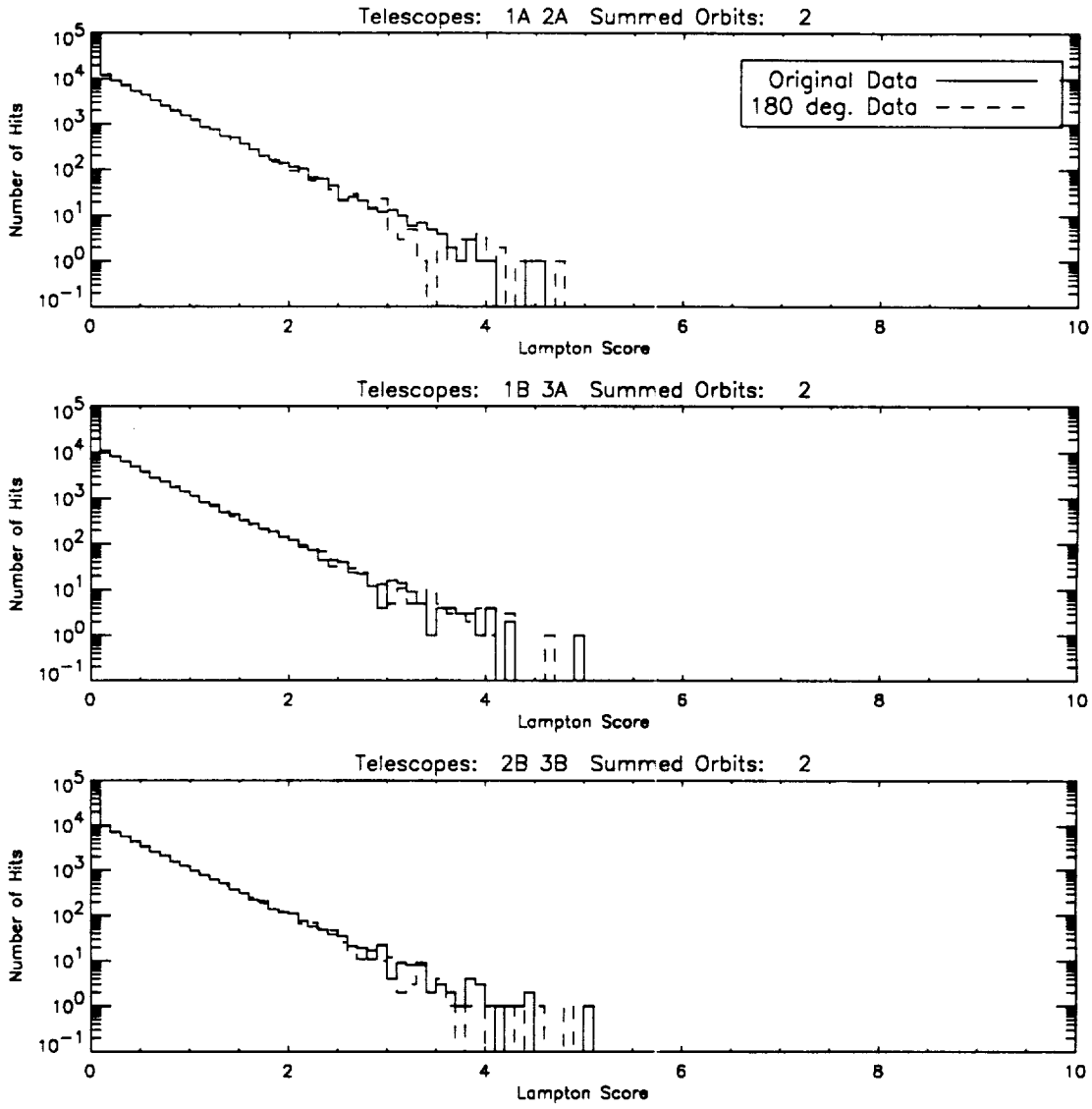

Figure 2: Comparison of Original and 180° Data: 2 Orbits Summed

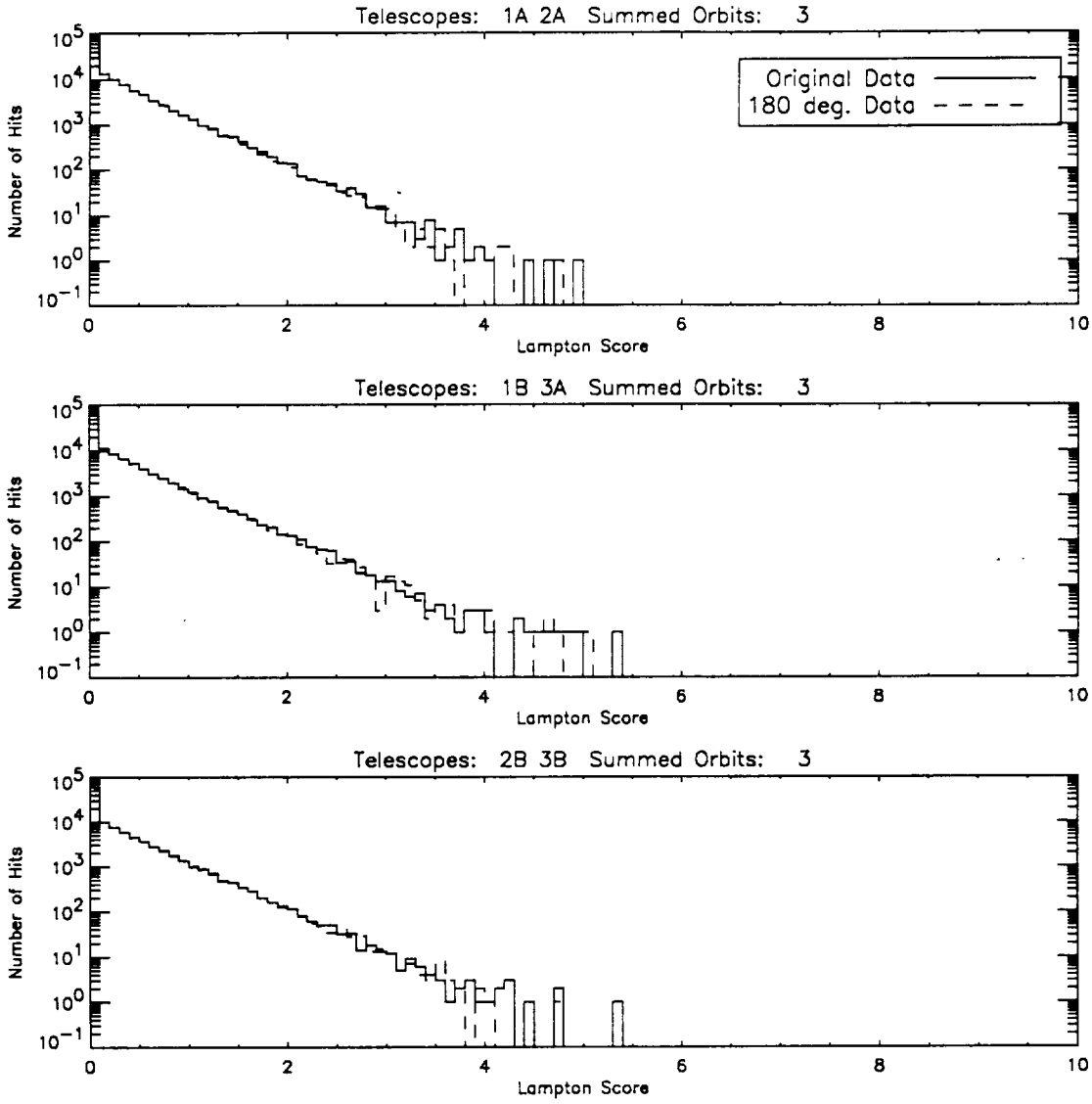

Figure 3: Comparison of Original and 180° Data: 3 Orbits Summed

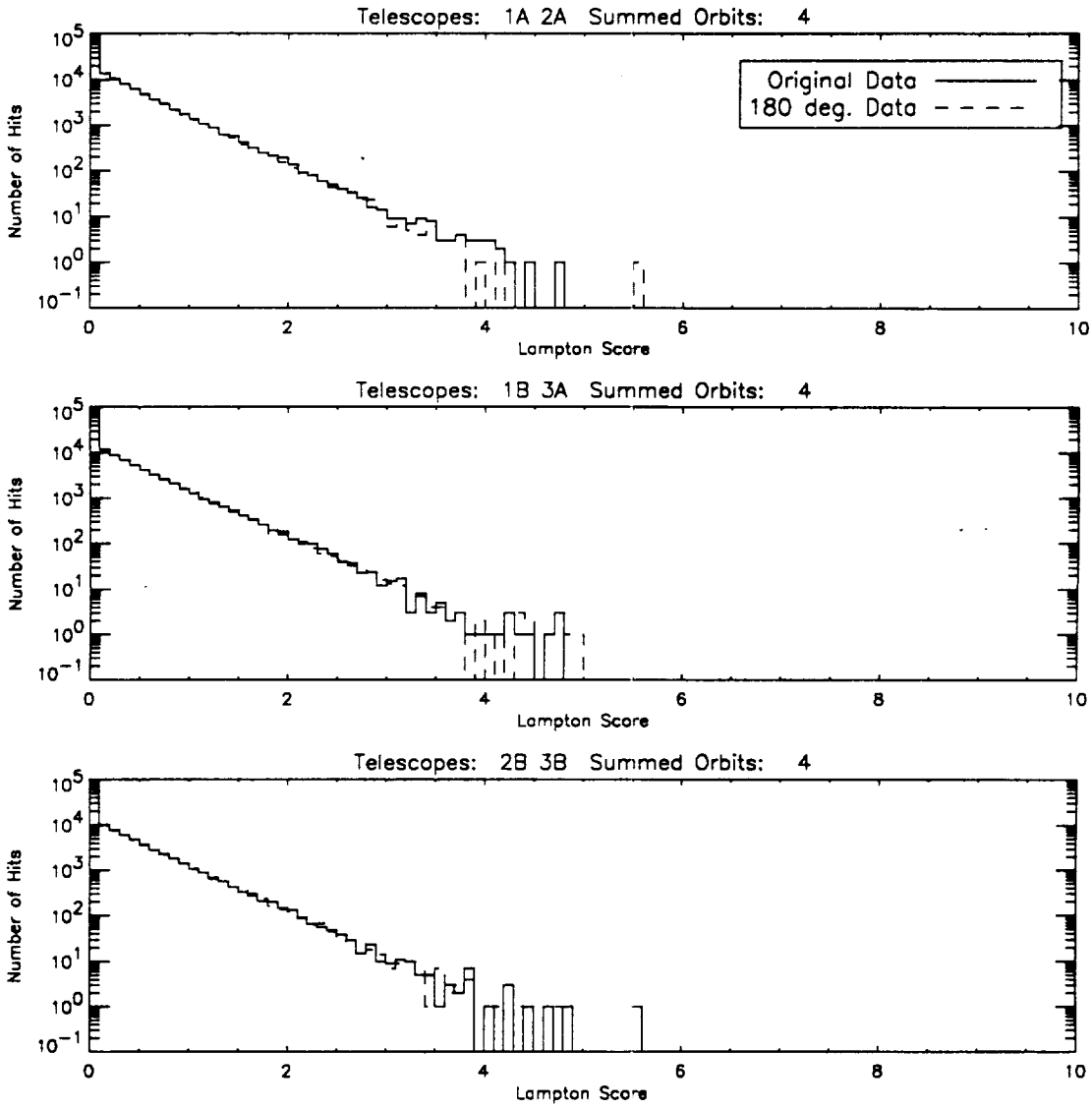

Figure 4: Comparison of Original and 180° Data: 4 Orbits Summed

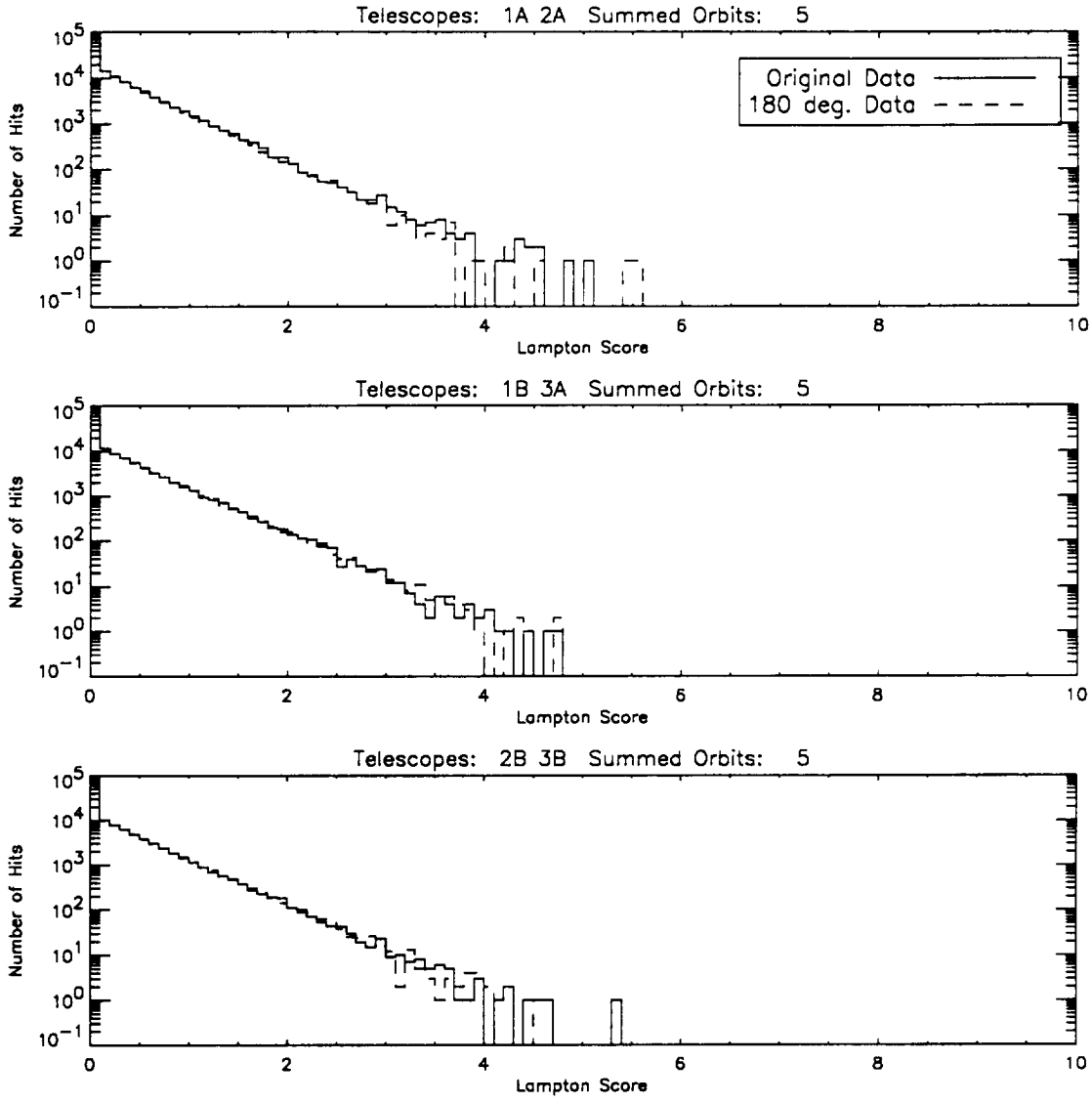

Figure 5: Comparison of Original and 180° Data: 5 Orbits Summed

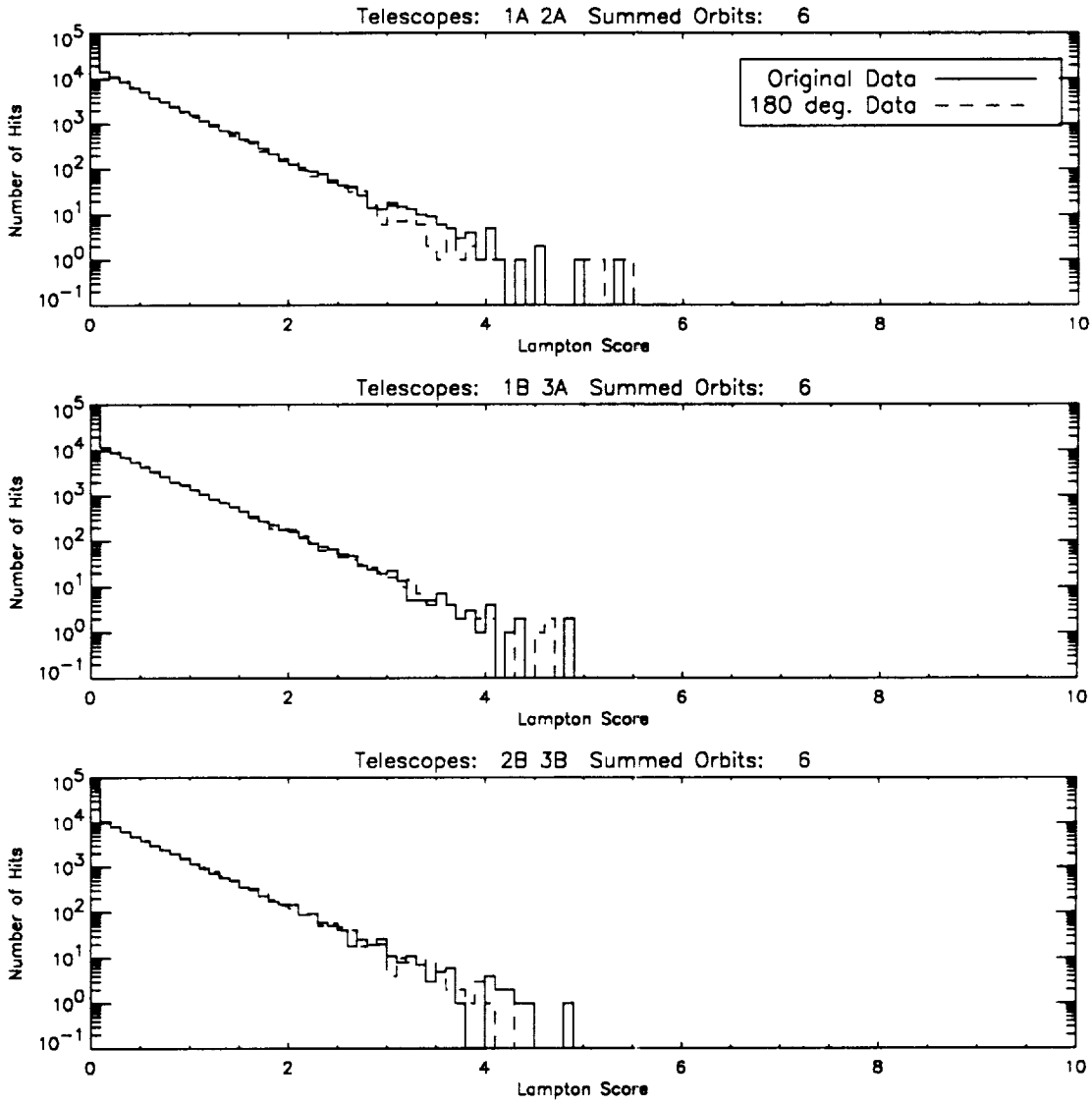

Figure 6: Comparison of Original and 180° Data: 6 Orbits Summed

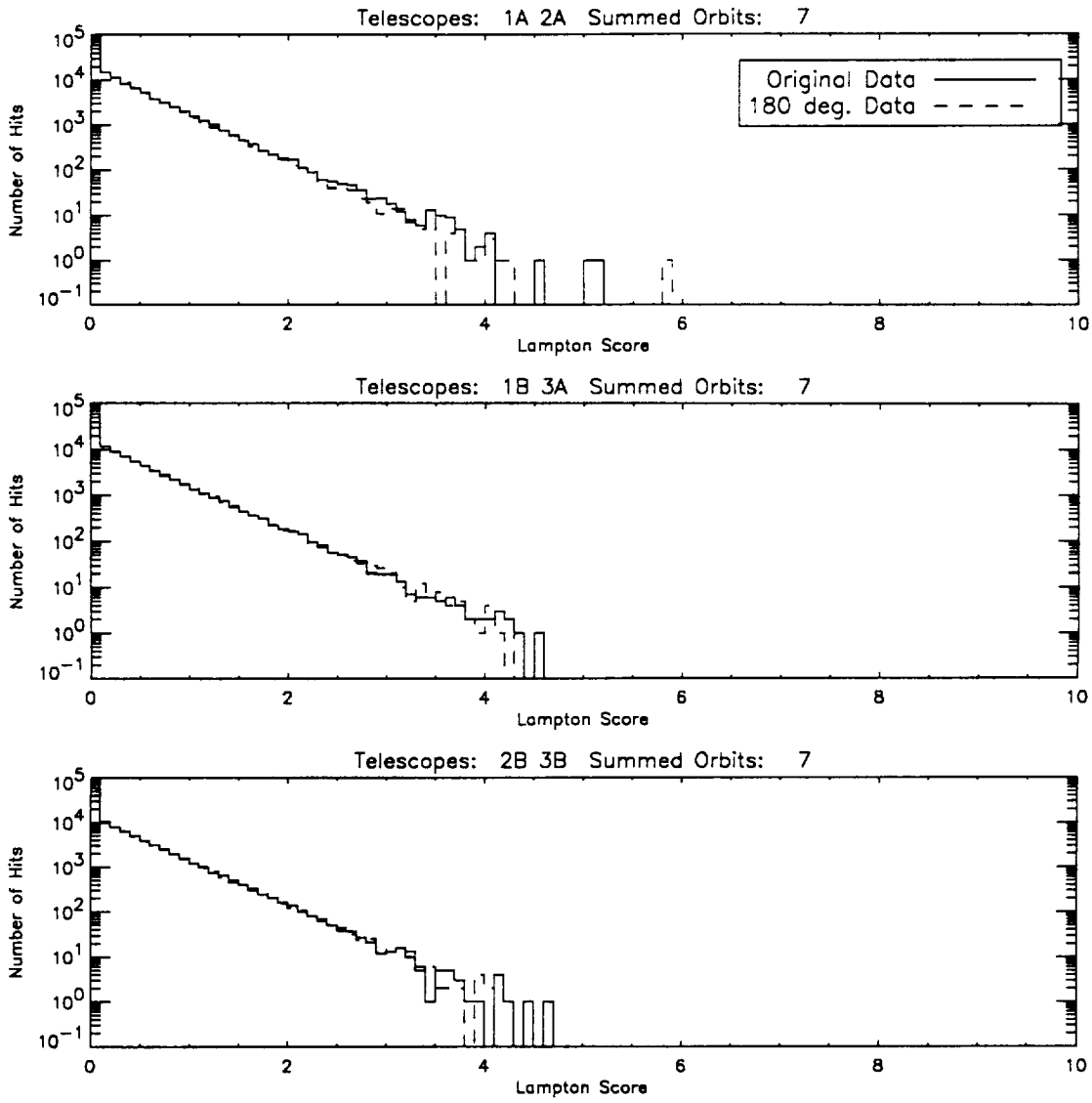

Figure 7: Comparison of Original and 180° Data: 7 Orbits Summed

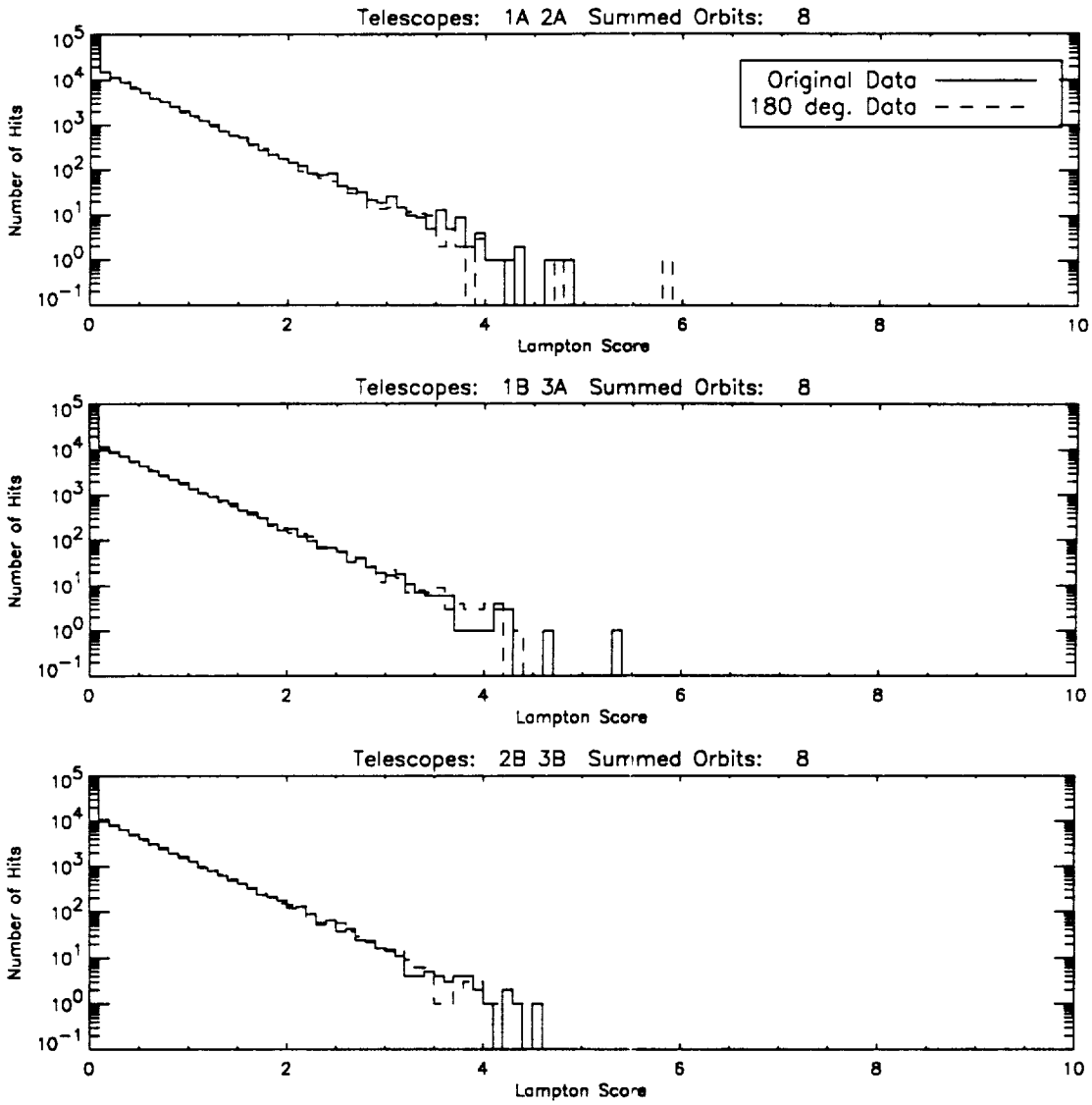

Figure 8: Comparison of Original and 180° Data: 8 Orbits Summed

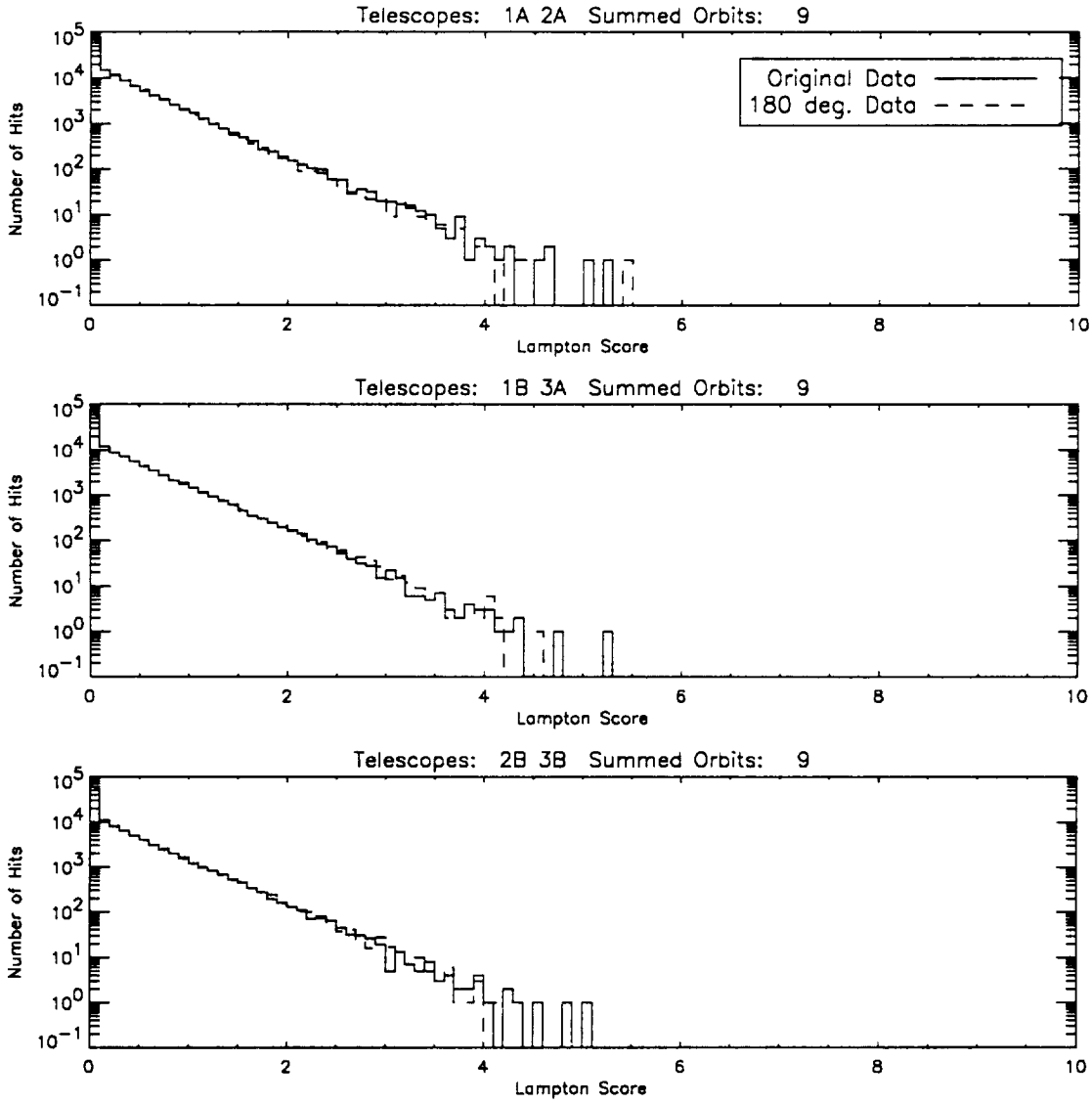

Figure 9: Comparison of Original and 180° Data: 9 Orbits Summed

Appendix B

Histograms of Summed Data Set

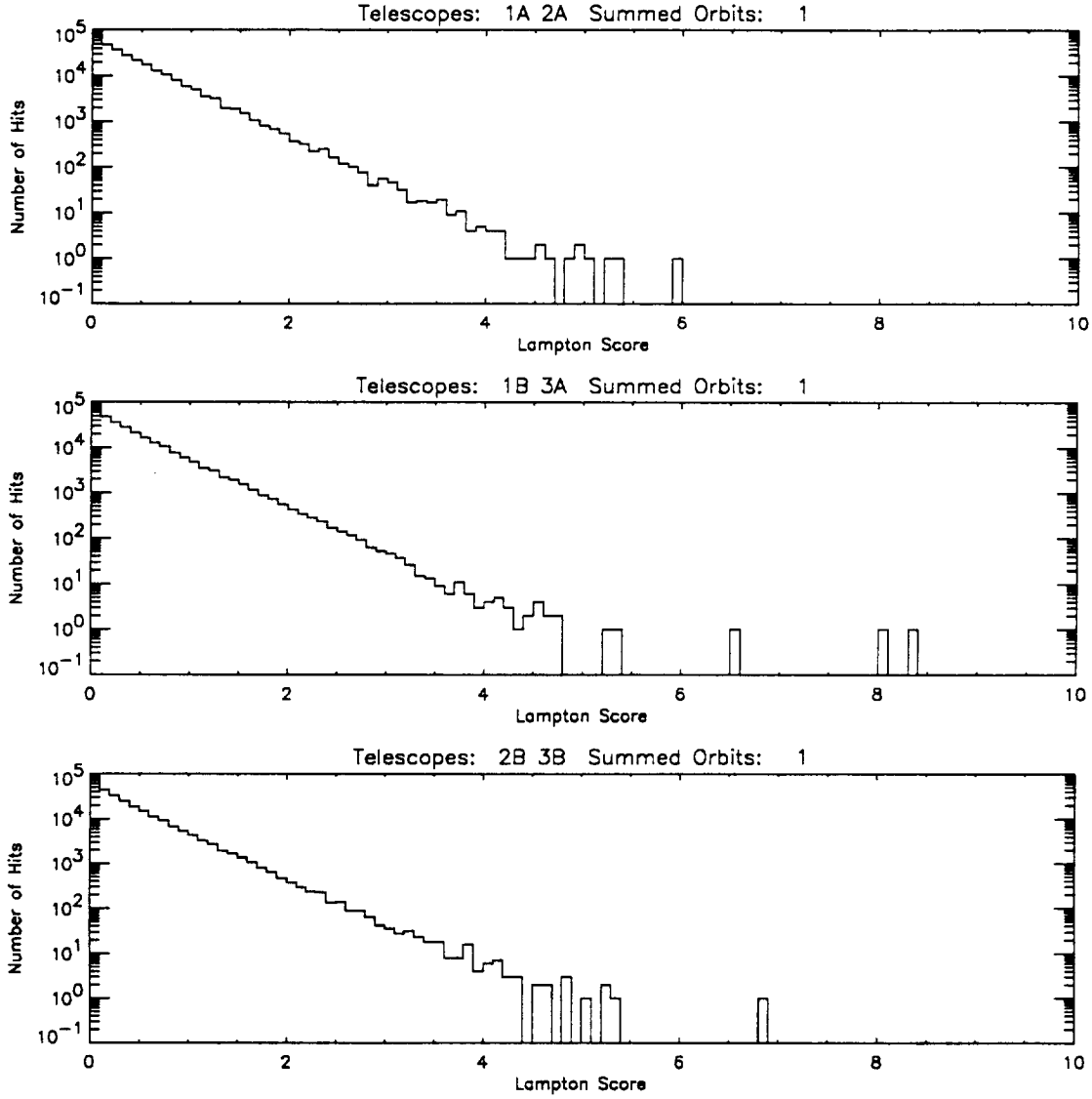

Figure 1: Histogram of Lampton Scores for All Data: 1 Orbits Summed

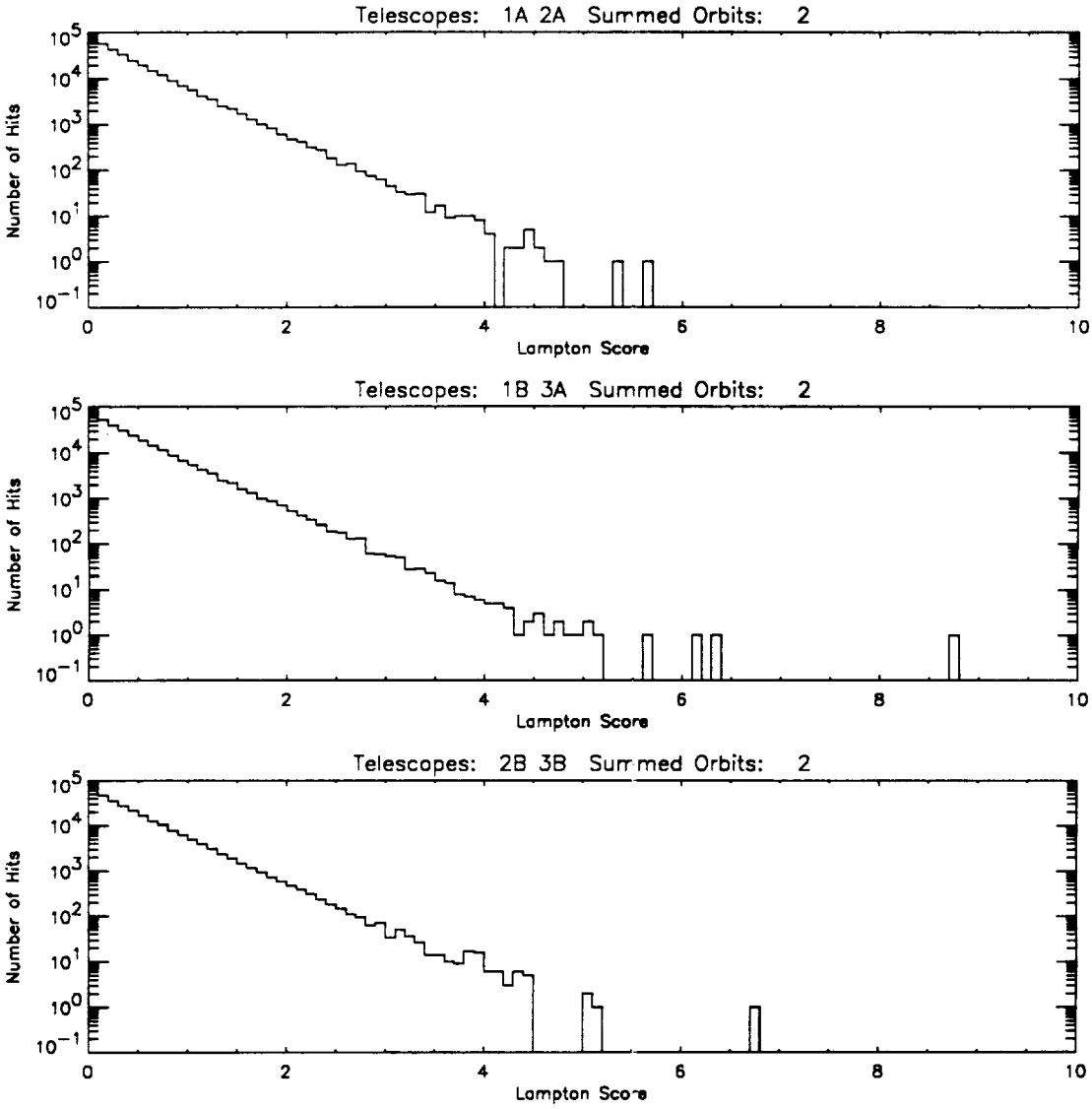

Figure 2: Histogram of Lampton Scores for All Data: 2 Orbits Summed

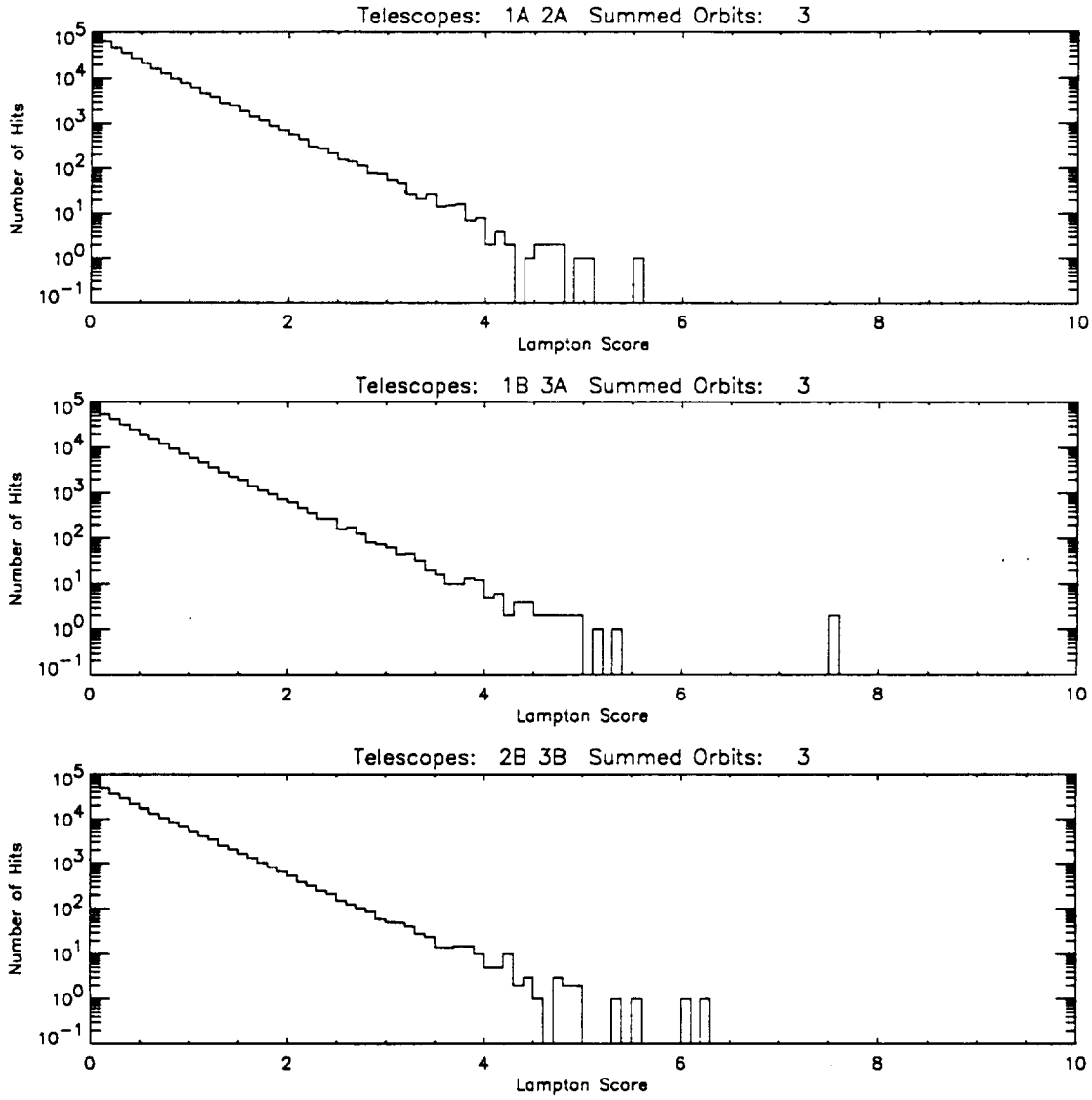

Figure 3: Histogram of Lampton Scores for All Data: 3 Orbits Summed

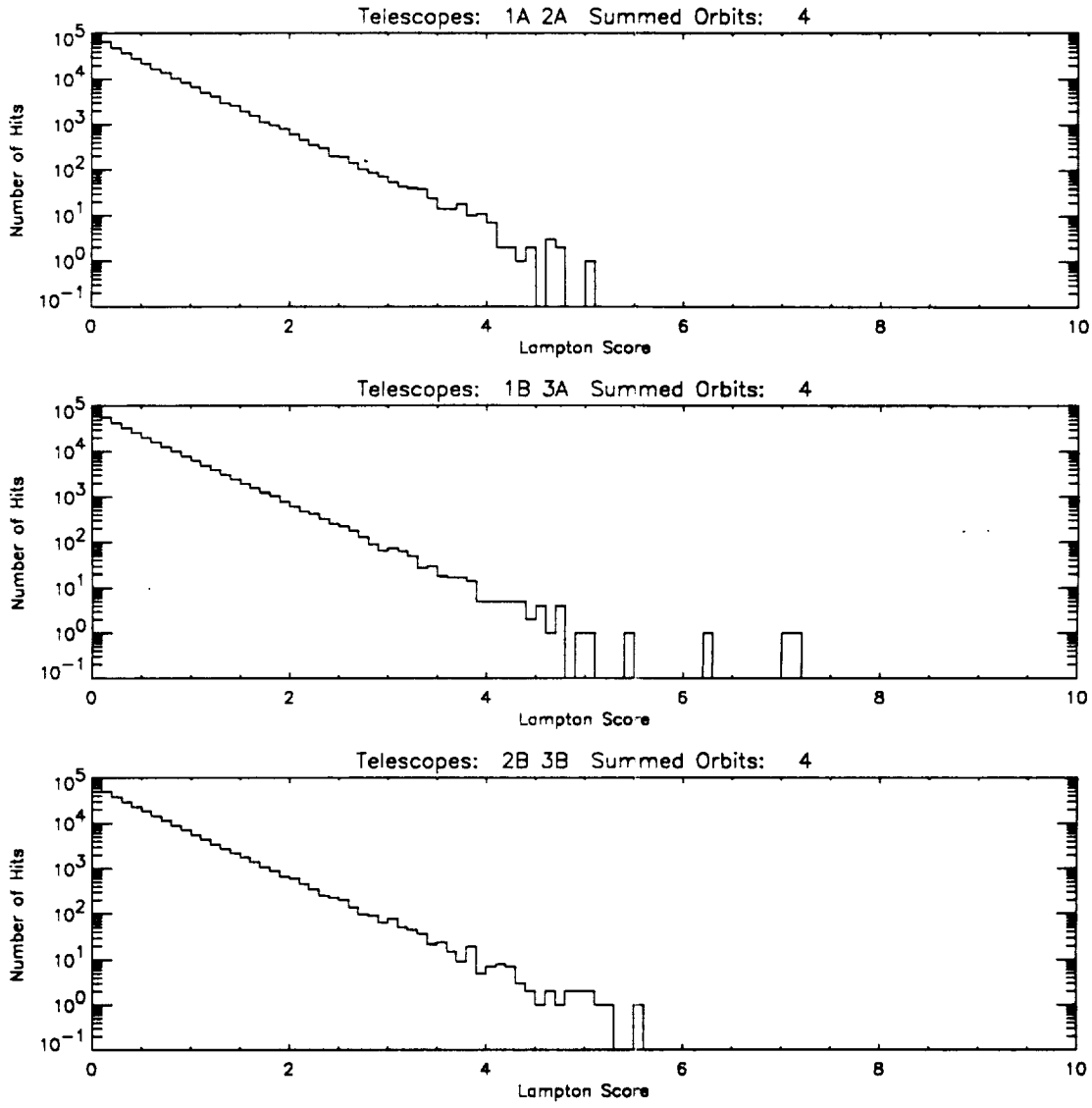

Figure 4: Histogram of Lampton Scores for All Data: 4 Orbits Summed

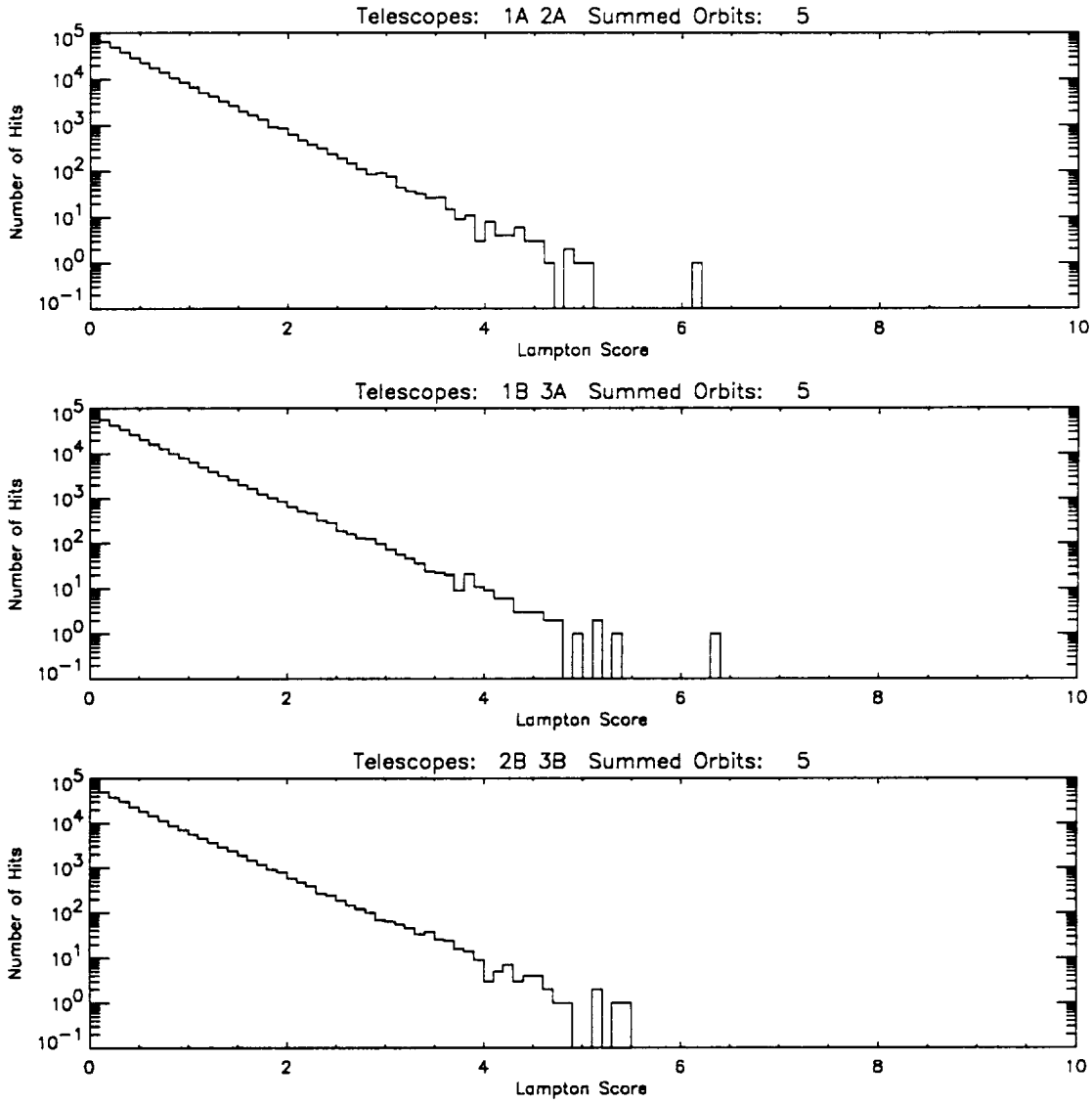

Figure 5: Histogram of Lampton Scores for All Data: 5 Orbits Summed

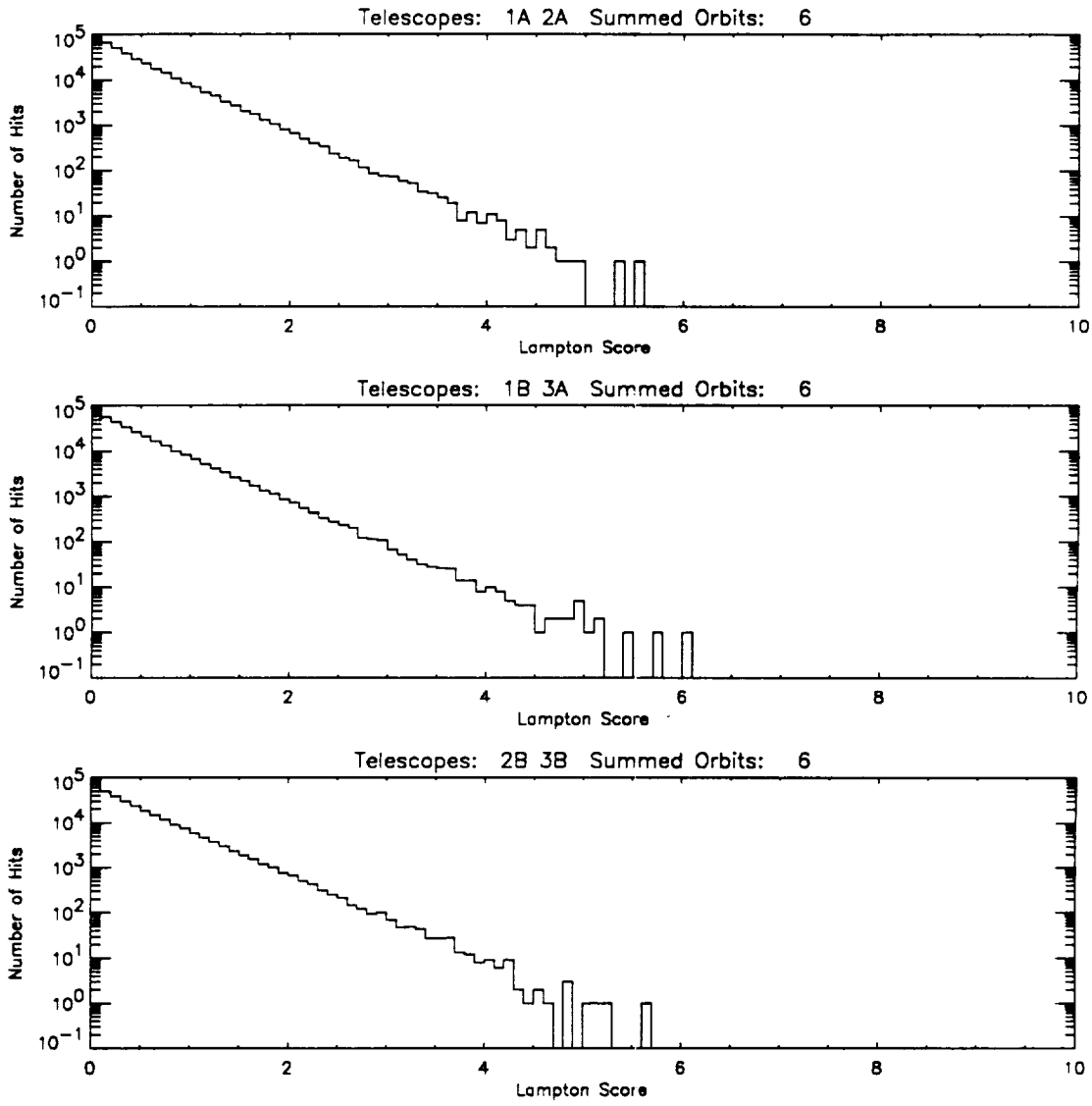

Figure 6: Histogram of Lampton Scores for All Data: 6 Orbits Summed

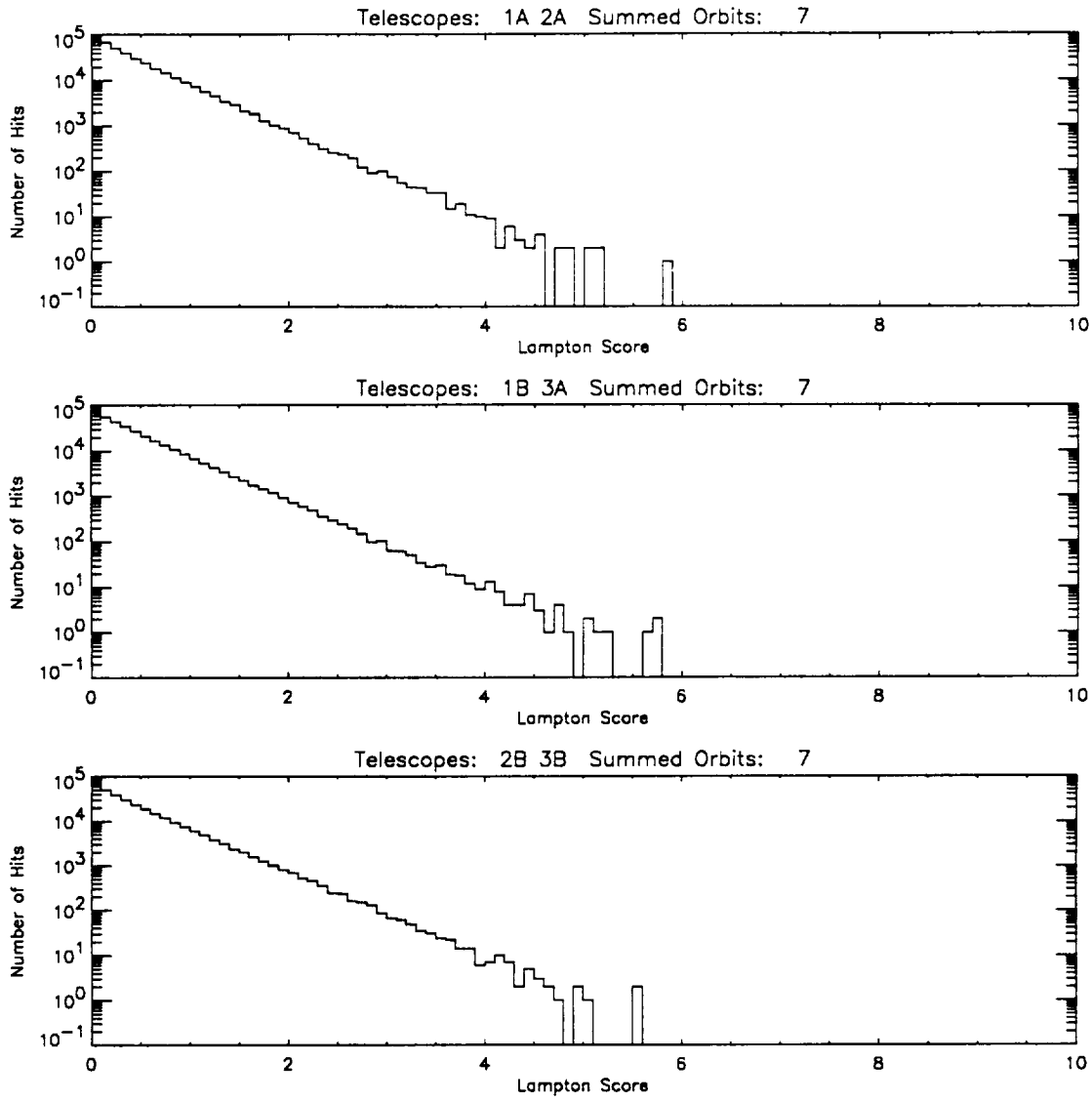

Figure 7: Histogram of Lampton Scores for All Data: 7 Orbits Summed

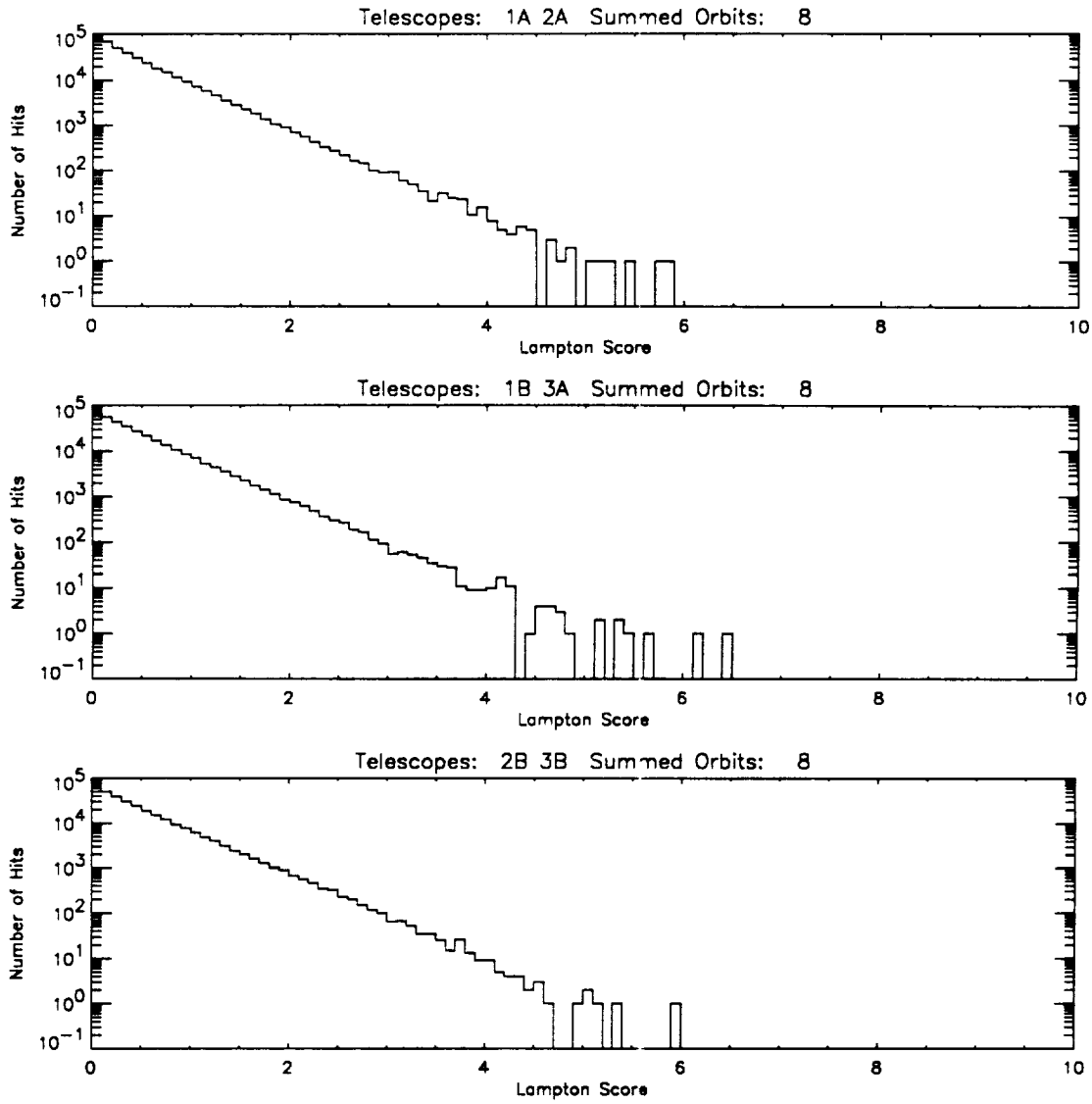

Figure 8: Histogram of Lampton Scores for All Data: 8 Orbits Summed

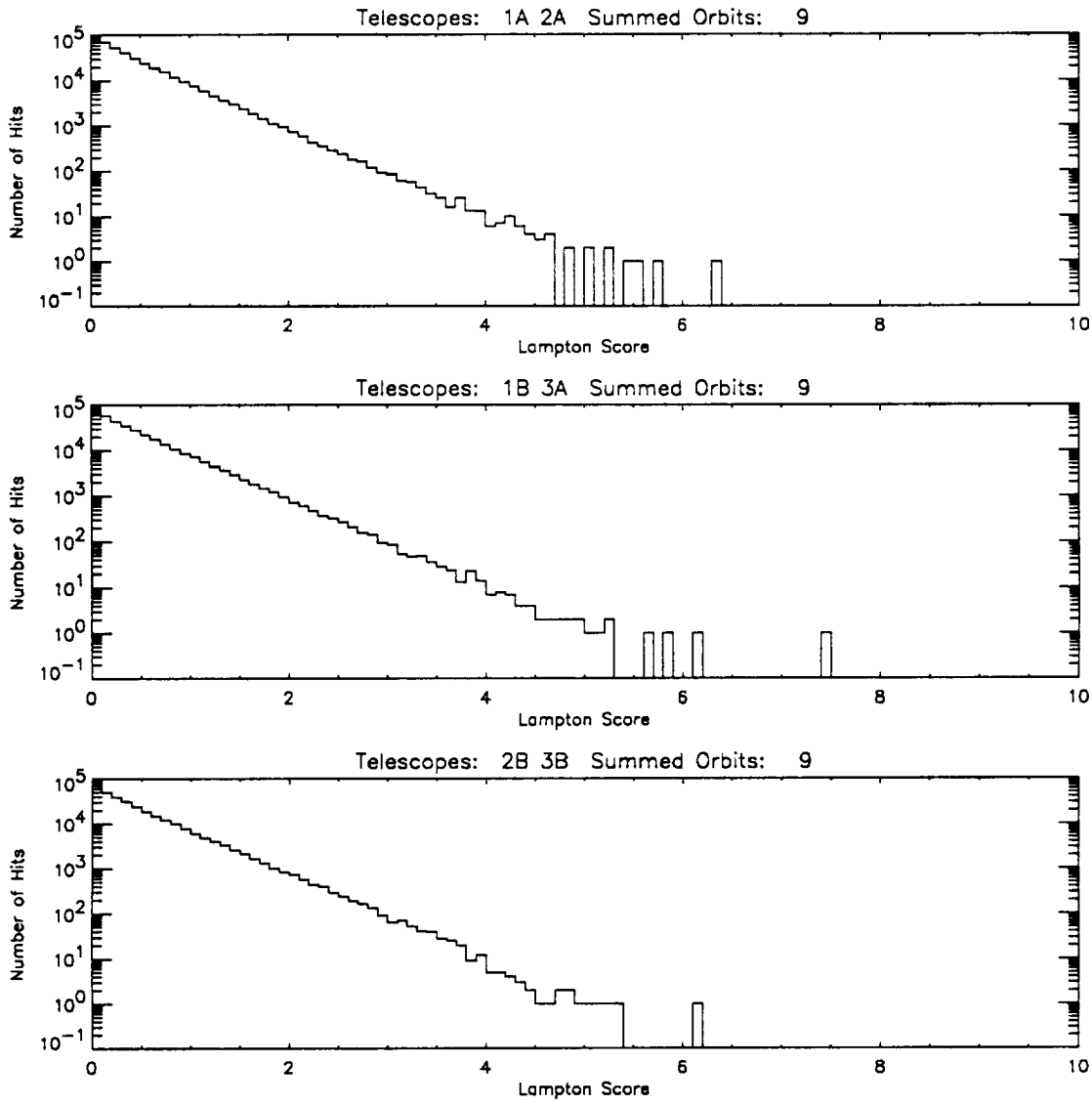

Figure 9: Histogram of Lampton Scores for All Data: 9 Orbits Summed

Appendix C

Target List

# RA (2000)	DEC	NAME	D(PC)	PER (D)	SP TYPE
107.515	38.543	Gl 268	5	10.428	dM5e/dM5e
169.545	31.529	xi UMa B	8	3.980	G5V
339.678	-20.623	FK Aqr	8	4.083	dM2e/dM3e
283.863	8.404	V1285 Aql	11	10.319	M3.5Ve/M3.5Ve
1.422	45.810	ADS 48A	11	0.000	dK6
223.349	19.153	HR 5553	12	125.369	K2V
96.543	18.757	OU Gem	12	6.992	K3V/K5V
38.591	-44.798	CC Eri	12	1.561	K7Ve/wdM4
79.173	45.998	alpha Aur	13	104.021	G1III/K0III
113.658	31.870	YY Gem	14	0.814	dM1e/dM1e
315.012	40.074	V1396 Cyg	15	3.276	M2V/M4Ve
298.573	-23.941	HR 7578	15	46.817	K2-3V/K2-3V
248.601	57.149	CM Dra	15	1.268	M4Ve/M4Ve
278.483	51.719	BY Dra	16	5.975	K4V/K7.5V
69.198	27.134	V833 Tau	17	1.788	dK5e
20.737	7.419	AR Psc	17	14.300	K2V/?
248.680	-4.219	Gl 629.2A	20	133.286	G5V
8.812	-3.593	13 Cet A	21	2.082	{F7V/}G4V
243.669	33.858	sigma2 CrB	21	1.140	F6V/G0V
42.182	31.115	VY Ari	21	13.198	K3-4V-IV
347.489	47.958	KZ And	23	3.033	dK2/dK2
174.320	47.453	DF UMa	23	1.034	dM0e/(dM5)
354.391	46.458	lambda And	23	20.521	G8IV-III
283.972	23.557	V775 Her	24	2.879	K0V/(K5-M2V
10.697	35.547	FF And	24	2.170	dM1e/dM1e

198.233	-59.817	HR 4980	25	4.233	G0V/G0V
354.879	28.246	KT Peg	25	6.202	G5V/K6V
110.090	-52.309	HR 2814	26	122.169	F9.5V{K3:V/(K5V
286.885	30.254	V478 Lyr	26	2.131	G8V/(dK-dM)
74.109	64.403	BD+64 487	27	44.380	K2V/K2V
140.608	40.201	BF Lyn	29	3.804	K2V/(dK)
185.549	73.248	AS Dra	29	5.413	G4V/G9V
358.767	28.634	II Peg	29	6.724	K2-3V-IV
320.256	40.345	HR 8170	29	3.243	F8V/wK5V
239.683	25.570	MS Ser	30	9.015	K2V/K6V
88.363	-43.558	SZ Pic	30	4.960	G8V
272.067	29.691	V815 Her	31	1.810	G5V/(M1-2V)
11.835	24.267	zeta And	31	17.769	/K1III
150.007	24.553	DH Leo	32	1.070	{K0V/K7V}K5V
61.884	-52.568	AG Dor	32	2.562	K1Vp
159.009	-11.909	LR Hya	34	6.866	K0V/K0V
325.386	-14.047	42 Cap	34	13.174	G2IV
302.112	15.675	BD+15 4057	34	5.434	G5V/G5V
67.155	19.741	vB 69	35	41.660	K0V
40.856	-37.928	UX For	35	0.955	G5-8V/(G)
54.197	0.588	V711 Tau	36	2.838	G5IV/K1IV
176.996	20.219	93 Leo	36	71.690	A6:V/G5IV-II
120.649	57.274	54 Cam	38	11.068	F9IV/G5IV
259.357	-66.949	V824 Ara	39	1.682	G5IV/K0V-IV
273.795	-32.789	CP-32 5229	40	0.000	K5Ve
63.108	23.675	BD+23 635	40	2.394	dK0/dM0:
271.457	21.447	ADS 11060C	42	25.762	K7:V/K7V
271.457	21.446	V772 Her	42	0.880	{G0V/ M1V }G5V
72.298	24.812	V808 Tau	42	11.929	K3V/K3V
65.684	15.056	BD+14 690	45	4.000	G0V
64.412	16.948	V818 Tau	45	5.609	G6V/K6V
64.507	18.257	BD+17 703	46	75.648	G4V/G8V
345.115	-33.743	TZ PsA	46	1.643	G5Vp
315.608	27.807	ER Vul	46	0.698	G0V/G5V
332.170	45.742	AR Lac	47	1.983	G2IV/K0IV
88.085	-57.156	HR 2072	48	0.000	F/G5-8III
51.647	28.715	UX Ari	50	6.438	G5V/K0IV
67.987	36.743	V492 Per	50	21.290	K1III
47.170	25.592	BD+25 497	50	6.150	G4V/G6V
343.260	16.841	IM Peg	50	24.650	K2III-II
319.645	11.569	BD+10 4514	50	3.966	{F9V/G0V}GIV
323.050	0.222	BD-00 4234	50	3.757	K3Ve/K7Ve

203.699	37.182	HR 5110	53	2.613	F2IV/K2IV
231.912	-63.020	LS TrA	54	49.431	K2IV/K2IV
13.243	-74.652	CF Tuc	54	2.798	G0V/K4IV
16.030	26.587	BD+25 161	55	91.900	G2V
187.420	24.521	BD+25 2511	55	3.558	<G9V>
54.296	25.991	V837 Tau	55	1.930	G2V/K5V
134.927	-27.816	TY Pyx	55	3.199	G5IV/G5IV
200.668	35.929	BD+36 2368	57	17.764	G5V
150.417	17.410	XY Leo B	58	0.805	M1V/M3V
57.549	17.255	V471 Tau	59	0.521	WD/K2V
115.828	28.884	sigma Gem	59	19.604	K1III
97.774	-59.004	TZ Pic	60	13.637	K1IV-IIIp
20.710	0.712	BI Cet	60	0.516	G5V:/G5V:
192.410	-6.078	BD-05 3578	60	1.309	G5V/(K-M)
74.571	0.454	V1198 Ori	60	0.000	G5IV
174.843	-39.384	CD-38 7259	62	11.710	G5V/K1IV
218.565	-60.408	V841 Cen	63	5.998	K1IV
314.559	35.175	CG Cyg	63	0.631	G9.5V/K3V
48.463	43.863	BD+43 657	65	45.779	G5IV
19.151	-2.500	AY Cet	67	56.824	WD/G5III
282.800	59.388	omicron Dra	67	138.420	G9III
337.527	49.356	V350 Lac	69	17.755	K2III
260.432	39.975	HR 6469	69	2018.000	{F2V/ G0V }G5IV
5.695	-9.230	BD Cet	71	35.100	K1III
251.492	82.037	epsilon UMi	71	39.481	A8-F0V/G5III
155.448	60.913	BD+61 1183	72	0.000	G8IV
100.328	82.267	SV Cam	74	0.593	G2-3V/K4V
62.420	-7.892	EI Eri	75	1.947	G5IV
33.093	30.303	6 Tri	75	14.734	F5/K0III
34.600	-71.474	BQ Hyi	77	18.379	G1:Vp
206.001	-61.366	V851 Cen	80	11.989	K2IV-III
335.636	30.358	BD+29 4645	80	45.284	F5-8/G8IV
77.611	-77.217	CP-77 196	82	19.310	K1IIIp
349.223	25.719	EZ Peg	83	11.660	G5V-IV/K0IV:
268.853	36.189	BD+36 2975	83	3.304	G6V/K1IV
88.067	-28.656	CD-28 2525	85	0.000	G1V
69.978	53.080	3 Cam	85	121.000	K0III
186.260	25.561	IL Com	86	0.962	F8V/F8V
263.172	74.227	29 Dra	88	905.900	WD/K0-2III
323.568	-13.484	AS Cap	93	49.137	K1III
282.622	33.488	1E1848+3325	95	0.000	G5V
290.450	4.558	1E1919+0427	95	0.800	G5V/K0III-I

347.792	53.026	RT And	95	0.629	F8V/K0V
126.310	-7.170	LU Hya	95	16.537	K1IV
307.401	-21.126	AT Cap	99	23.206	K2III
137.381	54.397	XY UMa	100	0.479	G3V/(K4-5V)
57.518	44.968	HR 1176	100	962.800	F2:V/G8III
269.529	15.139	Z Her	100	3.993	F4V-IV/K0IV
20.590	-56.731	CP-57 296	100	0.657	G6-8IV-IIIe
26.673	-24.016	UV For	100	15.050	K0IV
237.387	25.460	BD+25 2973	110	0.000	G0IV/
241.473	10.685	BD+11 2910	110	4.285	G8IV
91.987	-54.439	TY Pic	110	106.740	F/G8-K0III
1.334	-5.707	33 Psc	111	72.930	K0III
193.891	25.892	IN Com	125	1.994	G5IV-III
19.230	6.812	UV Psc	125	0.861	G4-6V/K0-2V
348.349	2.676	SZ Psc	125	3.966	F8IV/K1IV
50.913	4.882	HR 1023	125	287.201	G1III:
48.343	48.109	LX Per	130	8.038	G0IV/K0IV
163.931	60.469	DM UMa	130	7.495	K0-1IV-III
183.923	72.551	HR 4665	130	64.440	K1III/K1III
76.551	59.021	12 Cam	134	80.895	K0III
128.249	-34.663	HR 3385	135	45.130	K0III
2.050	-2.448	5 Cet	140	96.439	wF/K1III
174.873	-65.398	HR 4492	140	61.360	A0/K2-4III
89.269	49.030	HR 2054	140	83.190	G8III
70.941	-10.682	RZ Eri	143	39.283	Am/K0IV
47.664	-5.394	EL Eri	146	48.263	G8IV-III
175.192	51.998	RW UMa	150	7.328	F8IV/K0IV
331.236	47.235	HK Lac	150	24.428	F1V/K0III
84.268	11.035	HR 1908	160	0.000	K4III
172.604	46.658	EE UMa	160	74.874	K2III
135.241	26.680	WY Cnc	160	0.829	G5V/(wM2)
85.362	3.778	V1149 Ori	164	53.580	K1III
196.610	-4.846	BD-4 3419	165	20.000	K2IV-III
209.604	-1.660	BH Vir	166	0.817	F8V-IV/G2V
271.751	-48.247	V832 Ara	170	5200.000	WD/G8III
249.766	60.702	WW Dra	180	4.630	G2IV/K0IV
197.654	35.935	RS CVn	180	4.798	F4IV/G9IV
269.660	22.146	MM Her	190	7.960	G2/K0IV
114.072	-44.957	V344 Pup	190	11.761	K1III
61.278	22.497	CF Tau	200	2.756	F8
330.378	43.891	RT Lac	205	5.074	G5:/G9IV
294.910	-6.193	V1379 Aql	209	20.660	sdB/K0IV-III

290.660	-20.641	V4138 Sgr	210	13.048	K1III
230.857	-6.610	GX Lib	219	11.134	(G-KV)/K1III
85.165	-20.299	TW Lep	220	28.344	F6IV/K2III
228.387	38.568	SS Boo	220	7.606	G0V/K0IV
90.973	31.328	CQ Aur	220	10.621	F5/K1IV
183.336	-9.080	HU Vir	220	10.388	K0IV
127.658	2.283	GK Hya	220	3.587	F8/G8IV
79.630	75.947	BD+75 217	220	0.000	K0III
282.505	33.151	1E1848+3305	229	2.300	K0III-IV
294.762	30.582	1E1937+3027	229	9.527	K0III-IV
230.605	25.624	UV CrB	230	18.665	K2III
324.954	-16.007	AD Cap	250	2.960	G5-8IV-V/G5
266.493	39.322	HR 6626	250	99.557	K3III
200.385	38.880	BM CVn	250	20.625	K1III
287.107	52.426	HR 7275	250	28.590	K1IV-III
109.103	73.332	SS Cam	255	4.824	F5V-IV/K0IV-II
344.720	0.316	AZ Psc	260	47.121	K0III
141.203	-23.826	IL Hya	263	12.908	K1III
318.688	-31.183	BN Mic	265	63.090	K1IIIp
218.950	-18.038	RV Lib	270	10.722	G8IV/K3IV
305.388	32.314	BD+31 4046	275	38.787	K0III
272.599	33.403	PW Her	285	2.881	F8-G2/K0IV
194.766	47.151	BD+47 2007	285	0.000	F/K0III
253.233	-26.751	CD-26 11634	300	314.000	K0III
129.375	23.562	RU Cnc	300	10.173	F5IV/K1IV
330.147	-2.743	FF Aqr	300	9.208	sd0-B/G8IV-II
199.717	33.439	BL CVn	300	18.692	G-KIV/K0III
292.806	55.732	HR 7428	302	108.854	A2V/K2III-II
30.946	35.591	BD+34 363	310	23.982	K0III
257.607	48.966	V792 Her	310	27.537	F2IV/K0III
276.411	18.294	AW Her	315	8.801	G2/G8IV
301.509	-18.706	V4091 Sgr	340	16.887	K0III
237.873	72.125	RS UMi	350	6.169	G0/G-K
258.485	26.181	BD+26 2976	350	122.560	G5III
195.380	28.628	UX Com	350	3.642	G2/K1(IV)
234.512	29.487	RT CrB	360	5.117	G2/G5-8IV
105.826	-5.735	VV Mon	380	6.051	G2IV/K0IV
294.177	27.884	V1764 Cyg	390	40.142	F/K1III:
129.786	31.796	RZ Cnc	395	21.643	K1III/K3-4III
262.641	-33.654	V965 Sco	400	30.969	F2IV/K1III
292.008	-40.834	V4139 Sgr	417	45.180	K2-3III
322.085	-52.833	BH Ind	417	22.349	K1IIICNIVp

119.836	41.785	BD+42 1790	440	37.900	(dF)/G5III
237.782	11.273	1E1548.7+1125	500	5.000	K5V-IV
144.305	-42.021	IN Vel	500	52.270	K2IIIp
110.200	-5.259	AR Mon	525	21.208	G8III/K2-3III
233.309	-8.535	UZ Lib	550	4.768	wA8/K0III
204.033	-33.479	CD-32 9477	760	22.740	K2IIIp
100.192	9.823	W92/NGC2264	900	0.000	K0:IVp
346.372	26.009	KU Peg	950	1411.000	G8II
41.558	27.878	RS Ari	0	8.803	F8IV-V/G5IV
77.590	35.797	HP Aur	0	1.423	G8
248.023	30.386	GU Her	0	4.343	K0
306.909	14.336	BI Del	0	7.252	K0
334.603	69.861	WW Cep	0	1.534	K0